



1 **Title:** Fluorescent Bioaerosol Particle, Molecular Tracer, and Fungal Spore Concentrations during Dry
2 and Rainy Periods in a Semi-Arid Forest

3

4

5 **Authors:** Marie Ila GOSSELIN^{1,2}, Chathurika M Rathnayake³, Ian Crawford⁴, Christopher Pöhlker²,
6 Janine Fröhlich-Nowoisky², Beatrice Schmer², Viviane R. Després⁵, Guenter Engling⁶, Martin
7 Gallagher⁴, Elizabeth Stone³, Ulrich Pöschl², and J. Alex Huffman^{1*}

8

9 ¹Department of Chemistry and Biochemistry, University of Denver, Denver, Colorado, USA

10 ²Max Planck Institute for Chemistry, Multiphase Chemistry and Biogeochemistry Departments, Mainz,
11 Germany

12 ³Department of Chemistry, University of Iowa, Iowa City, IA 52246, USA

13 ⁴Centre for Atmospheric Science, SEAES, University of Manchester, Manchester, UK

14 ⁵Institute of General Botany, Johannes Gutenberg University, Mainz, Germany

15 ⁶Division of Atmospheric Sciences, Desert Research Institute, Reno, NV, USA

16

17 * Correspondence to: alex.huffman@DU.edu

18

19 **Abstract:**

20 Bioaerosols pose risks to human health and agriculture and may influence the evolution of mixed-phase
21 clouds and the hydrological cycle on local and regional scales. The availability and reliability of methods
22 and data on the abundance and properties of atmospheric bioaerosols, however, are rather limited. Here
23 we analyze and compare data from different real-time Ultraviolet Laser/Light Induced Fluorescence (UV-
24 LIF) instruments with results from a culture-based spore sampler and offline molecular tracers for
25 airborne fungal spores in a semi-arid forest in the Southern Rocky Mountains of Colorado. Commercial
26 UV-APS (Ultraviolet Aerodynamic Particle Sizer) and WIBS-3 (Wideband Integrated Bioaerosol Sensor,
27 Version 3) instruments with different excitation and emission wavelengths were utilized to measure
28 fluorescent aerosol particles (FAP) during both dry weather conditions and periods heavily influenced by
29 rain. Seven molecular tracers of bioaerosols were quantified by analysis of total suspended particle (TSP)
30 high-volume filter samples using High Performance Anion Exchange Chromatography with Pulsed
31 Amperometric Detection (HPAEC-PAD). From the same measurement campaign Huffman et al. (2013)
32 previously reported dramatic increases in total and fluorescence particle concentrations during and
33 immediately after rainfall and also showed a strong relationship between the concentrations of FAP and
34 ice nuclei (Huffman et al., 2013; Prenni et al., 2013). Here we investigate molecular tracers and show that
35 during rainy periods the atmospheric concentrations of arabitol ($35.2 \pm 10.5 \text{ ng m}^{-3}$) and mannitol ($44.9 \pm$
36 13.8 ng m^{-3}) were 3–4 times higher than during dry periods. During and after rain the correlations between
37 FAP and tracer mass concentrations were also significantly improved. Fungal spore number
38 concentrations on the order of 10^4 m^{-3} , accounting for 2–4% of TSP mass during dry periods and 17–23%
39 during rainy periods, were obtained from scaling the tracer measurements and from multiple analysis
40 methods applied to the UV-LIF data. Endotoxin concentrations were also enhanced during rainy periods,
41 but showed no correlation with FAP concentrations. Average mass concentrations of erythritol,
42 levoglucosan, glucose, and (1→3)- β -D-glucan in TSP samples are reported separately for dry and rainy
43 weather conditions. Overall, the results indicate that UV-LIF measurements can be used to infer fungal
44 spore concentrations, but substantial development of instrumental and data analysis methods seems
45 required for improved quantification.



46 1. Introduction

47 Primary biological aerosols particles (PBAP) are of keen interest within the scientific community,
48 partially because methods for their quantification and characterization are advancing rapidly (Huffman
49 and Santarpia, 2016; Sodeau and O'Connor, 2016). The term PBAP, or equivalently bioaerosol, generally
50 comprises several classes of airborne biological particles including viruses, bacteria, fungal spores, pollen
51 and their fragments (Després et al., 2012; Fröhlich-Nowoisky, 2016). Fungal spores are of particular
52 atmospheric interest because they can cause a variety of deleterious health effects in humans, animals,
53 and agriculture, and it has been shown that they can represent a significant fraction of total organic
54 aerosol emissions (Deguillaume et al., 2008; Gilardoni et al., 2011; Madelin, 1994), especially in tropical
55 regions (Elbert et al., 2007; Huffman et al., 2012; Pöschl et al., 2010; Zhang et al., 2010). Current
56 estimates of the atmospheric concentration of fungal spores range from 10^0 to more than 10^4 m⁻³
57 (Frankland and Gregory, 1973; Gregory and Sreeramulu, 1958; Heald and Spracklen, 2009; Hummel et
58 al., 2015; Sesartic and Dallafior, 2011). Fungal spores may also impact the hydrological cycle as giant
59 cloud condensation nuclei (GCCN) or as ice nuclei (IN) (Haga et al., 2013; Morris et al., 2013; Sesartic et
60 al., 2013). Additionally, several classes of bioaerosols and their constituent components, such (1→3)-β-
61 D-glucan and endotoxins, have been implicated in respiratory distress and allergies (Burger, 1990;
62 Douwes et al., 2003; Laumbach and Kipen, 2005; Pöschl and Shiraiwa, 2015). For example, asthma and
63 allergies have shown notable increases during thunderstorms due to elevated bioaerosol concentrations
64 (Taylor and Jonsson, 2004) especially when attributed to fungal spores (Allitt, 2000; Dales et al., 2003).
65

66 Molecular tracers have long been utilized as a means of aerosol source tracking (Schauer et al.,
67 1996; Simoneit and Mazurek, 1989; Simoneit et al., 2004). In recent years, analysis of molecular tracers
68 has been utilized for the quantification of PBAP in atmospheric samples and has been compared with
69 results from microscopy (Bauer et al., 2008a) and culture samples (Chow et al., 2015b; Womiloju et al.,
70 2003). Three organic molecules have been predominately utilized as unique tracers of fungal spores:
71 ergosterol, mannitol, and arabitol. The majority of atmospherically relevant fungal spores are released by
72 active wet discharge processes common in *Ascomycota* and *Basidiomycota*, meaning that the fungal
73 organism actively ejects spores at a time most advantageous for the spore dispersal and germination
74 processes, often when relative humidity (RH) is high (Ingold, 1971). While there are several mechanisms
75 of active spore emission (e.g. Buller's drop (Buller, 1909) and osmotic pressure canons (Ingold, 1971)),
76 they each involve the secretion of fluid containing hygroscopic compounds, such as arabitol, mannitol,
77 potassium, chloride, and other solutes (Elbert et al., 2007), released near the site of spore growth. When
78 the spores are ejected, some of the fluid adheres to the spores and becomes aerosolized. Several of these
79 secreted compounds are thought to enter the atmosphere linked uniquely with spore emission processes,
80 and so these tracers have been used to estimate atmospheric concentrations of fungal spores. Arabitol and
81 mannitol are both sugar alcohols (polyols) that serve as energy stores for the spore (Feofilova, 2001).
82 Arabitol is unique to fungal spores and lichen, while mannitol is present in fungal spores, lichen, algae,
83 and higher plants (Lewis and Smith, 1967). Ergosterol is found within the cell membranes of fungal
84 spores (Weete, 1973) and can be used as an ambient fungal spore trace (Di Filippo et al., 2013; Miller and
85 Young, 1997). Comparing the seasonal trends of arabitol and mannitol with ergosterol, Burshtein et al.
86 (2011) showed positive correlations between arabitol or mannitol and ergosterol only in the spring and
87 autumn suggesting that the source of these polyols is unlikely to be solely fungal in origin or that the
88 amount of each compound emitted varies considerably between species type and season. While ergosterol
89 has been directly linked to fungal spores in the air, ergosterol is prone to photochemical degradation and
90 is difficult to analyze and quantify directly. Quantification of ergosterol typically requires chemical
91 derivatization by silylation before analysis via gas chromatography (Axelsson et al., 1995; Burshtein et
92 al., 2011; Lau et al., 2006). In contrast, analysis of sugar alcohols by ion chromatography involves fewer
93 steps and has been successfully applied to monitor seasonal variations of atmospheric aerosol
94 concentration at a number of sites (Bauer et al., 2008a; Caseiro et al., 2007; Yang et al., 2012; Yttri et al.,
95 2011a; Zhang et al., 2010; Zhang et al., 2015) including pg m⁻³ levels in the Antarctic (Barbaro et al.,
96 2015). By measuring spore count and tracer concentration in parallel at one urban and two suburban sites



97 in Vienna, Austria, Bauer et al. (2008a) estimated the amount of each tracer per fungal spore emitted.
98 Potassium ions have also been linked to emission of biogenic aerosol (Pöhlker et al., 2012b) and are co-
99 emitted with fungal spores, however, application of potassium as a fungal tracer is uncommon because it
100 is predominantly associated with biomass burning (Andreae and Crutzen, 1997). Additionally, (1→3)-β-
101 D-glucan (fungal spores and pollen) and endotoxins (gram-negative bacteria) have also been widely used
102 to measure other bioaerosols (Andreae and Crutzen, 1997; Cheng et al., 2012; Stone and Clarke, 1992).
103

104 The direct detection of PBAP has historically been limited to analysis techniques that require
105 culturing or microscopy of the samples. These systems are time-consuming, costly, and often
106 substantially undercount biological particles by an order of magnitude or more (Gonçalves et al., 2010;
107 Pyri and Kapsanaki-Gotsi, 2007). The sampling methods associated with these measurements also offer
108 relatively low time resolution and low particle size resolution. Recently, techniques utilizing ultraviolet
109 laser/light-induced fluorescence (UV-LIF) for the real-time detection of PBAP have been developed and
110 are being utilized by the atmospheric community for bioaerosol detection. Thus far, the most widely
111 applied LIF instruments for ambient PBAP detection have been the Ultraviolet Aerosol Particle Sizer
112 (UV-APS; TSI Inc. Model 3314, St. Paul, MN) and the Wideband Integrated Bioaerosol Sensor (WIBS;
113 University of Hertfordshire, Hertfordshire, UK, now licensed to Droplet Measurement Technologies,
114 Boulder, CO, USA). Both of these commercially available instruments can provide information in real-
115 time about particle size and fluorescence properties of supermicron atmospheric aerosols.
116 Characterization and co-deployment of these instruments over the past ten years has expanded the
117 knowledge base regarding how to analyze and utilize the information provided from these instruments
118 (Healy et al., 2014; Huffman et al., 2013; Pöhlker et al., 2013; Pöhlker et al., 2012a), though the
119 interpretation of UV-LIF results from individual particles is complicated by interfering material that is not
120 biological in nature (Gabey et al., 2010; Huffman et al., 2012; Lee et al., 2010; Saari et al., 2013; Toprak
121 and Schnaiter, 2013).
122

123 Here we present analysis of atmospheric concentrations of arabinitol and mannitol in relation to
124 results from real-time, ambient particle measurements reported by UV-APS and WIBS. We interrogate
125 these relationships as they pertain to rain conditions (rainfall and RH) that have previously been shown to
126 increase fluorescent aerosol concentration (Crawford et al., 2014; Huffman et al., 2013; Prenni et al.,
127 2013; Schumacher et al., 2013). Active wet discharge of ascospores and basidiospores has frequently
128 been reported to correspond with increased RH (Elbert et al., 2007), and fungal spore concentration has
129 also been shown to increase after rain events (e.g. Jones and Harrison, 2004). Here we estimate airborne
130 fungal concentrations in a semi-arid forest environment utilizing a combination of real-time fluorescence
131 methods, molecular fungal tracer methods, and direct-to-agar sampling and culturing as parallel
132 surrogates for spore analysis. This study represents the first ambient comparison of real-time aerosol UV-
133 LIF instruments with results from molecular tracers or culturing.
134

135 2. Methods

136 2.1 Sampling site

137 Atmospheric sampling was conducted as a part of the BEACHON-RoMBAS (Bio-hydro-
138 atmosphere interactions of Energy, Aerosols, Carbon, H₂O, Organics, and Nitrogen – Rocky Mountain
139 Biogenic Aerosol Study) field campaign conducted at the Manitou Experimental Forest Observatory
140 (MEFO) located 48 km northwest of Colorado Springs, Colorado (2370 m elevation, 39° 06' 0" N, 105°
141 5' 03" W) (Ortega et al., 2014). The site is located in the central Rocky Mountains and is representative of
142 semi-arid montane pine forested regions of North America. During BEACHON-RoMBAS, a large team
143 of international researchers conducted an intensive set of measurements from 20 July to 23 August 2011.
144 A summary of results from the campaign are published in the BEACHON campaign special issue of
145



146 Atmospheric Chemistry and Physics¹. All the data used in this study were gathered from instruments and
147 sensors located within a <100 m radius (e.g. Fig. 1).

148

149 2.2 Online fluorescent instruments

150 A UV-APS and WIBS-3 (Model 3; University of Hertfordshire) were operated continuously as a
151 part of the study, and particle data were integrated to five-minute averages before analysis. The UV-APS
152 was operated under procedures defined in previous studies (Huffman et al., 2013; Schumacher et al.,
153 2013). A total suspended particle (TSP) inlet head ~5.5 m above ground, mounted above the roof of a
154 climate-controlled, metal trailer, was used to sample aerosol directed towards the UV-APS. Bends and
155 horizontal stretches in the 0.75 inch tubing were minimized to reduce losses of large particles (Huffman et
156 al., 2013). The UV-APS detects particles between 0.5-20 μm and records aerodynamic particle diameter
157 and integrated total fluorescence (420-575 nm) after pulsed excitation by a 355 nm laser (Hairston et al.,
158 1997). Both UV-APS and WIBS instruments report information about particle number concentration, but
159 it is instructive here to show results in particle mass for comparison between all techniques. Total particle
160 number size distributions (irrespective of fluorescence properties) obtained from the UV-APS were
161 converted to mass distributions using unit particle mass density of as a first approximation for all direct
162 comparisons with tracer mass and unless otherwise stated. Total particle concentration values (in $\mu\text{g m}^{-3}$)
163 were obtained for each five-minute period by integrating over the size range 0.5 – 15 μm , and these mass
164 concentration values were averaged over the length of the filter sampling periods. Uncertainty in mass
165 concentration values reported here is influenced by utilizing a single, estimated value for particle mass
166 density and because of slight dissimilarities between UV-APS and WIBS instruments in size binning at
167 particle sizes above 10 μm that dominate particle mass.

168

169 A WIBS-3 was used to continuously sample air at a site ~50 m away from the UV-APS trailer
170 and 1.3 m above the ground. Briefly, the diameter of individual particles sampled by the WIBS is
171 estimated by the intensity of the elastic side-scatter from a continuous wave 635 nm diode laser and
172 analyzed by a Mie scattering model (Foot et al., 2008; Kaye et al., 2005). Particles that pass through the
173 diode laser activate two optically-filtered Xenon flash lamps. The first lamp excites the particle at 280 nm
174 and the second at 370 nm. Emission from the 280 nm excitation is filtered separately for two PMTs, one
175 which detects in a band at 310-400 nm and the other in a band at 410-650 nm. These excitation and
176 emission wavelengths result in a total of three channels of detection: λ_{ex} 280 nm, λ_{em} 320 – 400 nm (FL 1
177 or Channel A); λ_{ex} 280 nm, λ_{em} 410 – 650 nm (FL 2 or Channel B); and λ_{ex} 370 nm, λ_{em} 410– 650 nm (FL
178 3 or Channel C) (Foot et al., 2008; Gabey et al., 2010; Perring et al., 2015). Individual particles are
179 considered fluorescent here if they exceed fluorescent thresholds for any channel, as defined as the
180 average of a “forced trigger” baseline plus 3 standard deviations (σ) of the baseline measurement (Gabey
181 et al., 2010).

182

183 WIBS particle-type analysis is utilized to define types of particles that have specific spectral
184 patterns. As defined by Perring et al. (2015), the 3 different fluorescent channels (FL1, FL2, and FL3) can
185 be combined to produce 7 unique fluorescent categories. Observed fluorescence in channel FL1 alone, but
186 without any detectable fluorescence in Channel FL2 or FL3, categorizes a particle as type A. Similarly,
187 observed fluorescence in channels FL2 or FL3, but in no other channels, places a particle in the B or C
188 categories, respectively. Combinations of fluorescence in these channels, such as a particle that exhibits
189 fluorescence in both FL1 and FL2 categorizes a particle as type AB and so on for a possible seven particle
190 types as summarized in Figure S1.

191

192 As a separate tool for particle categorization, the University of Manchester has recently
193 developed and applied a hierarchical agglomerative cluster analysis tool for WIBS data, which they have

¹http://www.atmos-chem-phys.net/special_issue247.html



194 applied to the BEACHON-RoMBAS campaign (Crawford et al., 2014; Crawford et al., 2015; Robinson et
195 al., 2013). Here we utilize clusters derived from WIBS-3 data as described by Crawford et al. (2015).
196 Cluster data presented here was analyzed with the Open Source Python package FastCluster (Mullner,
197 2013). Briefly, hierarchical agglomerative cluster analysis was applied to the entire data set and each
198 fluorescent particle was uniquely clustered into one of 4 groups. Cluster 1, assigned by Crawford et al.
199 (2015) as fungal spores, displayed a 1.5-2 μm mode and a daily peak in the early morning that paralleled
200 relative humidity (Schumacher et al., 2013). Clusters 2, 3, and 4 have strong, positive correlations with
201 rainfall and exhibit size modes that peak at $<1.2 \mu\text{m}$ and were initially described by Crawford et al. as
202 bacterial particles. Here we have summed Clusters 2-4 to a single group referred to as Cl_{Bact} , for
203 simplicity when comparing with molecular tracers.

204

205

206

207

208

209

210

211

212

213

214

215

216

217

218

219

220

221

222

223

224

225

226

227

228

229

230

231

232

233

234

235

236

237

238

239

240

241

242

243

244

The WIBS-3 utilized here has since been updated to the WIBS-4 (Univ. Hertfordshire, UK) and
WIBS-4A (Droplet Measurement Technologies, Boulder, Colorado). One important difference between
the models is that the WIBS-3 exhibits comparatively weak FL1 and FL2 signals with respect to the more
updated models, and is thus more influenced by FL3. This results in a different break-down of channel
intensity between instrument models, as will be discussed later.

2.3 High volume sampler

Total suspended particle samples were collected for molecular tracer and molecular genetic
analyses using a high volume sampler (Digital DHA-80) drawing 1000 L min^{-1} through 15 cm glass fiber
filters (Macherey-Nagel GmbH, Type MN 85/90, 406015, Düren, Germany) over a variety of sampling
times ranging from 4-48 h (supplemental Table S1). The sampler was located $<50 \text{ m}$ from each of the
UV-LIF instruments described here, approximately between the WIBS-3 and UV-APS. Prior to sampling
all filters were baked at $500 \text{ }^\circ\text{C}$ for 12 h to remove DNA and organic contaminants. Samples were stored
in pre-baked aluminum bags after sampling at $-20 \text{ }^\circ\text{C}$ for 1-30 days and then at $-80 \text{ }^\circ\text{C}$ after overnight,
international transport cooled on dry ice. Due to the low vapor pressure of the molecular tracers analyzed
loss due to volatilization is considered unlikely (Zhang et al., 2010). 36 samples were collected during the
study, in addition to handling field blanks and operational field blanks. Handling blanks were acquired by
placing a filter into the sampler and immediately removing, without turning on the air flow control.
Operational blanks were placed into the sampler and exposed to 10 seconds of air flow.

2.4 Slit Sampler

A direct-to-agar slit sampler (Microbiological Air Sampler STA-203, New Brunswick Scientific
Co, Inc., Edison, NJ) was used to collect culturable airborne fungal spores. The sampler was placed $\sim 2 \text{ m}$
above ground on a wooden support surface with 5 cm x 5 cm holes to allow air flow both up and down
through the support structure. Sampled air was drawn over the 15 cm diameter sampling plate filled with
growth media at a flow rate of 28 L min^{-1} for sampling periods of 20 to 40 min. Growth media (malt
extract medium) was mixed with antibacterial agents (40 units streptomycin, Sigma Aldrich; 20 units
ampicillin, Fisher Scientific) to suppress bacterial colony growth. Plates were prepared several weeks in
advance and stored in a refrigerator at ca. $4 \text{ }^\circ\text{C}$ until used for sampling. Before each sampling period, all
surfaces of the samplers were sterilized by wiping with isopropyl alcohol. Handling and operational
blanks were collected to verify that no fungal colonies were being introduced by handling procedures. 14
air samples were collected over 20 days and immediately moved to an incubator (Amerex Instruments,
Incumax IC150R) set at $25 \text{ }^\circ\text{C}$ for 3 days prior to counting fungal colonies formed. Each colony, present
as a growing dot on the agar surface, is assumed to have originated as one colony forming unit (CFU; i.e.
fungal spore) deposited onto the agar by impaction during sampling. The atmospheric concentration of
CFU per air volume was calculated using the sampler air flow. Further discussion of methods and initial
results from the slit sampler were published by Huffman et al. (2013).

2.5 Offline filter analyses

245 *2.5.1 Carbohydrate analysis*

246 Approximately 1/8 of each frozen filter was cut for carbohydrate analysis using a sterile
247 technique, meaning that scissors were cleaned and sterilized and cutting was performed in a positive-
248 pressure laminar flow hood. In order to precisely determine the fractional area of the filter to be analyzed,
249 filters were imaged from a fixed distance above using a camera and compared to a whole, intact filter.
250 Using ImageJ software (Rasband and ImageJ, 1997), the area of each filter slice showing particulate
251 matter (PM) deposit was referenced to a whole filter, and thereby the amount of each filter utilized could
252 be determined. This technique allowed for an estimate of the fraction of each sampled used for the
253 analysis, which corresponds to the fraction of PM mass deposited. The uncertainty on the filter area
254 fraction is estimated at 2%. The uncertainty was determined as the percent of variation in the area of the
255 filter edge (no PM deposit) as compared to the total filter area.

256
257 Carbohydrates were extracted from quartz filter samples and analyzed following the procedure
258 described by Rathnayake et al. (2016). A total of 36 samples were analyzed along with field and lab
259 blanks. All lab and field blanks fell below method detection limits. Extraction was performed by placing
260 the filter slice into a centrifuge tube that had been pre-rinsed with Nanopure™ water (resistance > 18.2
261 MΩ cm⁻¹; Barnstead EasyPure II, 7401). A volume of 8.0 mL of Nanopure™ water was added to the filter
262 in the centrifuge tube to extract water-soluble carbohydrates. Samples were then exposed to rotary
263 shaking for 10 min at 125 rpm, sonication for 30 min at 60 Hz (Branson 5510, Danbury, CT, US), and
264 rotary shaking for 10 min. After shaking, the extracted solutions were filtered through a 0.45 μm
265 polypropylene syringe filter (GE Healthcare, UK) to remove insoluble particles, including disintegrated
266 filter pieces. One 1.5 mL aliquot of each extracted solution was analyzed for carbohydrates within 24
267 hours of extraction. A duplicate 1.5 mL aliquot was stored in a freezer and analyzed, if necessary due to
268 lack of instrument response and invalid calibration check, within 7 days of extraction. Analysis of
269 carbohydrates was done using a High Performance Anion Exchange Chromatography System with Pulsed
270 Amperometric Detection (HPAEC-PAD, Dionex ICS 5000, Thermo Fisher, Sunnyvale, CA, USA).
271 Details of the instrument specifications and quality standards for carbohydrate determination are available
272 in Rathnayake et al. (2016). Calibration curves for mannitol, levoglucosan, glucose (Sigma-Aldrich),
273 arabitol and erythritol (Alfa Aesar) were generated with seven points each, ranging in aqueous
274 concentration from 0.005 ppm to 5 ppm. The method detection limits for mannitol, levoglucosan, glucose,
275 arabitol and erythritol were 2.3, 2.8, 1.6, 1.0 and 0.6 ppb, respectively. Method detection limits were
276 determined as 3σ of analyte concentrations recovered from seven spiked filter samples (Rathnayake et al.,
277 2016). All calibration curves were checked daily using a standard solution to ensure all concentration
278 values were within 10% of the known value. Failure to maintain a valid curve resulted in recalibration of
279 the instrument.

280
281 *2.5.2 DNA analysis*

282 Methods and initial results from DNA analysis from these high volume filters were published by
283 Huffman et al. (2013). Briefly, fungal diversity was determined by previously optimized methods for
284 DNA extraction, amplification, and sequence analysis of the internal transcribed spacer regions of
285 ribosomal genes from the high volume filter samples (Fröhlich-Nowoisky et al., 2012; Fröhlich-
286 Nowoisky et al., 2009). Upon sequence determination, fungal sequences were compared with known
287 sequences using the Basic Local Alignment Search Tool (BLAST) at the National Center for
288 Biotechnology (NCBI) and identified to the lowest taxonomic rank common to the top BLAST hits after
289 chimeric sequences had been removed. When sequences displayed >97% similarity, they were grouped
290 into operational taxonomic units (OTUs).

291
292 *2.5.3 Endotoxin and glucan analysis*

293 Sample preparation for quantification of endotoxin and (1→3)-β-D-glucan included extraction of
294 5 punches (0.5 cm² each) of the quartz filters with 5.0 mL of pyrogen-free water (Associates of Cape Cod
295 Inc., East Falmouth, MA, USA), utilizing an orbital shaker (300 rpm) at room temperature for 60 min,



296 followed by centrifuging for 15 min (1000 rpm). One-half mL of supernatant was submitted to a kinetic
297 chromogenic limulus amoebocyte lysate (Chromo-LAL) endotoxin assay (Associates of Cape Cod Inc.,
298 East Falmouth, MA, USA) using a ELx808IU (BioTek Instrument Inc., Winooski, VT, USA) incubating
299 absorbance microplate reader. For (1→3)-β-D-glucan measurement, 0.5 mL of 3 N NaOH was added to
300 the remaining 4.5 mL of extract and the mixture was agitated for 60 min. Subsequently, the solution was
301 neutralized to pH 6–8 by addition of 0.75 mL of 2 N HCl. After centrifuging for 15 min (1→3)-β-D-
302 glucan concentration was determined in the supernatant using the GlucateLL® LAL kinetic assay
303 (Associates of Cape Cod, Inc., East Falmouth, MA). The minimum detection limits (MDLs) and
304 reproducibility were 0.046 Endotoxin Units (EU) m⁻³ and ± 6.4% for endotoxin and 0.029 ng m⁻³ and ±
305 4.2% for (1→3)-β-D-glucan, respectively. Laboratory and field blank samples were analyzed as well,
306 with lab blank values being below detection limits, while field blank values were used to subtract
307 background levels from sample data. More details about the bioassays can be found elsewhere (Chow et
308 al., 2015a).

309

310 2.6 Meteorology and wetness sensors

311 Meteorological data were recorded by a variety of sensors located at the site. Precipitation was recorded
312 by a laser optical disdrometer (PARTICLE SIZE and VELOCITY “PARSIVEL” sensor; OTT Hydromet
313 GmbH, Kempton, Germany) and separately by a tipping bucket rain gauge. The disdrometer provides
314 precipitation occurrence, rate, and physical state (rain or hail) by measuring the magnitude and duration
315 of disruption to a continuous 780 nm laser that was located in a tree clearing (Fig. 1), while the tipping
316 bucket rain gauge measures a set amount of precipitation before tipping and triggering an electrical pulse.
317 A leaf wetness sensor (LWS; Decagon Devices, Inc., Pullman, WA), provided a measurement of
318 condensed moisture by measuring the voltage drop across a leaf surface to determine a proportional
319 amount of water on or near the sensor. Additional details of these measurements can be found in Huffman
320 et al. (2013) and Ortega et al. (2014).

321

322 3. Results and Discussion

323

324 3.1 Categorization and characteristic differences of Dry and Rainy periods

325 Increases in PBAP concentration have been frequently associated with rainfall (e.g. Bigg et al.,
326 2015; Faulwetter, 1917; Hirst and Stedman, 1963; Jones and Harrison, 2004; Madden, 1997). Fungal
327 polyols have also been reported to increase after rain and have been used as indicators of increased fungal
328 spore release (Liang et al., 2013; Lin and Li, 2000; Zhu et al., 2015). Recently it was shown that the
329 concentration of fluorescent aerosol particles (FAP) measured during BEACHON-RoMBAS increased
330 dramatically during and after periods of rain (Crawford et al., 2014; Huffman et al., 2013; Schumacher et
331 al., 2013) and that these particles were associated with high concentrations of ice nucleating particles that
332 could influence the formation and evolution of mixed-phase clouds (Huffman et al., 2013; Prenni et al.,
333 2013; Tobo et al., 2013). It was observed that a mode of smaller fluorescent particles (2–3 μm) appeared
334 during rain episodes, and several hours after rain ceased a second mode of slightly larger fluorescent
335 particle (4–6 μm) emerged, persisting for up to 12 h (Huffman et al., 2013). The first mode was
336 hypothesized to result from mechanical ejection of particles due to rain splash on soil and vegetated
337 surfaces, and the second mode was suggested as actively emitted fungal spores (Huffman et al., 2013).
338 While the UV-APS and WIBS each provide data at high enough time resolution to see subtle changes in
339 aerosol concentration, the temporal resolution of the chemical tracer analysis was limited to 4–48 h
340 periods defined by the collection time of the high volume sampler. To compare the measurement results
341 across the sampling platforms, UV-LIF measurements were averaged to the lower time resolution of the
342 filter sampler periods, and the periods were grouped into three broad categories: Rainy, Dry, and Other, as
343 will be defined below.

344 Time periods were wetness-categorized in two steps: first at 15 min resolution and then averaged
345 for each individual filter sample. During the first stage of categorization each 15 min period was
346 categorized into one of four groups: rain, post-rain, dry, or other. To categorize each filter period, an



347 algorithm was established utilizing UV-APS fluorescent particle fraction and accumulated rainfall. The
348 ratio of integrated number of fluorescent particles to total particles was used as a proxy for the increased
349 emission of biological particles. Figure 2a presents a time series of the size-resolved fluorescent particle
350 concentration, showing increases during rain periods in dark red. A relatively consistent diurnal cycle of
351 increased FAP concentration in the 2-4 μm range is apparent almost every afternoon, which corresponds
352 to near daily afternoon rainfall during approximately the first half of the measurement period.
353 Disdrometer and tipping bucket rainfall measurements were each normalized to unity and summed to
354 produce a more robust measure of rainfall rate, because it was observed that often only one of the two
355 systems would record a given light rain event. If a point was described by total rainfall accumulation
356 greater than 0.201 it was flagged as rain. A point was flagged as post-rain if it immediately followed a
357 rain period and also exhibited a fluorescent particle fraction greater than 0.08. The purpose of this
358 category was to reflect the observation that sustained, elevated concentrations of FAP persisted for many
359 hours even after the rain rate, RH, and leaf wetness returned to pre-rain values. The only measurement
360 that adequately reflected this scenario was of the fluorescent particles measured by UV-APS and WIBS
361 instruments. The post-rain flag was continued until the fluorescent particle fraction fell below 0.08 or if it
362 started to rain again (with calculated rain values greater than 0.201). Points were flagged as dry periods if
363 they exhibited rainfall accumulation and fluorescent particle fraction below the thresholds stated above.
364 Several periods were not easily categorized by this system and were considered in a fourth category as
365 other. This occurred when fluorescent particle fraction above the threshold value was observed with no
366 rainfall.

367
368 Once wetness categories were assigned by the algorithm at 15 min resolution, each high volume
369 filter sample was categorized by a similar nomenclature, but using only three categories. These were
370 defined as Dry, Rainy (combination of rain and post rain categories), or Other based on the relative time
371 fraction in each of the four original 15 min categories. For each sample, if the relative time fraction of a
372 given category exceeded 0.50 the sample was assigned to that category. Despite the effort to categorize
373 samples systematically, several sample periods (5 of 35) appeared mis-categorized by looking at FAP
374 concentration, rainfall, RH, and leaf wetness in more detail. In some circumstances, this was because light
375 rainfall produced observable increases in FAP, but without exceeding the rainfall threshold. Or in other
376 circumstances a period of rainfall occurred at the very end or just before the beginning of a sample, and so
377 the many-hour period was heavily influenced by aerosol triggered by a period of rain just outside of the
378 sample time window. As a result, several samples were manually re-categorized as described here.
379 Samples 20 and 21 (Table S1) were four-hour samples that displayed high relative humidity and rainfall,
380 thus samples were originally characterized as Rainy. This period was described by an extremely heavy
381 rain downpour (7.5 mm in 15 min), however, that seemingly placed the samples in a different regime of
382 rain-aerosol dynamics than the other Rainy samples and so these two samples were moved to the Other
383 category. Sample 23, originally Rainy, presented a FAP fraction marginally above the 0.08 threshold, but
384 visually displayed a trend dissimilar to other post-rain periods and so was re-categorized as Dry. Sample
385 28 showed no obvious rainfall, but the measurement team observed persistent fog in three consecutive
386 mornings (Samples 25, 27, 28), and the concentration of fluorescent (2-6 μm) particles suggested a source
387 of particles not influenced by rain, and so this Rainy sample was re-categorized as Other. Sample 38
388 displayed a fluorescent number ratio just below the threshold value, and was thus categorized as Dry,
389 however, the measurement team observed post-rain periods at the beginning and end of the sample, so the
390 sample were re-categorized as Other. For all samples other than these five, the categorization was
391 determined using the majority (> 0.50) of the 15 min periods. In no cases other than the five that were re-
392 categorized was the highest category fraction less than 0.50 of the sample time. Note that we have chosen
393 to capitalize Rainy, Dry, and Other to highlight that we have rigorously defined the period using the
394 characterization scheme described above and to separate the nomenclature from the general, colloquial
395 usage of the terms. Wetness category assignment for each high volume filter sample period is shown in
396 Figure 2 as a background color (brown for Dry samples, green for Rain-influenced samples, and pink for
397 Other samples) and Table S1.



398

399

400 To validate the qualitative differences between wetness categories described in the last section,
401 we present observations about each of these groupings. First, we organized the WIBS data according to
402 the particle categories introduced by Perring et al. (2015). By this method, every fluorescent particle
403 detected by the WIBS can be defined uniquely into one of seven categories (i.e. A, AB, ABC and so on).
404 By plotting the relative fraction of fluorescent particles described by each particle type, temporal
405 differences between measurement periods can be observed, as shown in Figure 2e. To a first
406 approximation, this analysis style allows for coarse discrimination of particle types. For example, a given
407 population of particles would ideally exhibit a consistent fraction of particles present in the different
408 particle categories as a function of time. By this reasoning, sample periods categorized as Dry (most of
409 the latter half of the study; brown bars in Fig. 2) would be expected to have a self-consistent particle type
410 trend, whereas sample periods categorized as Rainy (most of the first half of the study; green bars in Fig.
411 2) would have a self-consistent particle type trend, but different from the Dry samples. This is broadly
412 true. During Rainy periods as seen in Figure 3a, there is a relatively high fraction (> 65%) of ABC
413 particles (light blue) and a relatively low fraction (< 15%) in BC (purple) and C (yellow) type particles,
414 suggesting heavy influence from the FL1 channel. In contrast, during Dry periods the fraction of ABC
415 particles (light blue) is reduced (<25%) while BC (purple) and C (yellow) type particles increase in
416 relative fraction (>30% and >40%, respectively) suggested a diminished influence of FL1 channel.

417

418 It is important to note a few important caveats here. First, the ability of the WIBS to discriminate
419 finely between PBAP types is relatively poor and it is still unclear exactly how different particle types
420 would appear by this analysis method. Particles of different kinds and from different sources are likely
421 convolved into a single WIBS particle type, which could either soften or enhance the relationships with
422 rain discussed here. Second, the assignment of particle types is heavily size-dependent and sensitive to
423 subtle instrument parameters, and so it is unclear how different instruments would present similar particle
424 types. For example, Hernandez et al. (2016) used two WIBS instruments and found differences in relative
425 fraction of particle categories for samples aerosolized in the lab. They reported fungal spores to be
426 predominately A, AB, and ABC type particles, whereas Rainy sample periods suggested to have heavy
427 fungal spore influence by Huffman et al. (2013) show predominantly C, BC, and ABC particle fraction.
428 These discrepancies may be due to the comparison of ambient particles to laboratory-grown cultures. The
429 highly controlled environment of a laboratory may not always accurately represent the humidity
430 conditions in which fungal spore release occurs in this forest setting (Saari et al., 2015). This would
431 impact the fluorescence properties of the fungal spore particles which are inhibited by increased moisture
432 level around the spore (Hill et al., 2009). More likely, however, is that the WIBS-3 used here exhibits
433 higher sensitivity in the FL3 channel with respect to the FL1 and FL2 channels (Robinson et al., 2013), as
434 compared to the WIBS-4A used one of the units reported by Hernandez et al. (2016). This would explain
435 the shift here towards particles with C-type fluorescence. One piece of evidence for this is the quantitative
436 comparison of particle measurements presented by the UV-APS and WIBS-3 instruments co-deployed
437 here (Fig. 4). The number concentration of particle exhibiting fluorescence above the FL2 baseline of the
438 WIBS-3 is approximately consistent with the number of fluorescent particles measured by the UV-APS,
439 and significantly below the concentration of FL3 particles. The UV-APS number concentration shows the
440 highest correlation with the WIBS FL2 channel: during Rainy periods, $R^2=0.70$; Dry, $R^2=0.82$; Other, $R^2=0.92$.
441 These observations are in stark contrast to the trends reported by Healy et al. (2014) that the UV-
442 APS fluorescent particle concentration correlated most strongly with the WIBS-4 FL3 and that the
443 number concentration of FL3 was the lowest out of all three channels. Given that the FL3 channel of the
444 WIBS and the UV-APS probe cover similar excitation and emission wavelengths it is expected that these
445 two channels should correlate well. Based on these data, we suggest that the WIBS-3 utilized here may
446 present a very different particle type break-down than if a WIBS-4 had been used. So, while caution is
447 recommended when comparing the relative break-down of WIBS particle categories shown here (Fig. 3)
448 with other studies, the data are internally self-consistent, and comparing qualitative differences between,
e.g. Rainy and Dry periods is expected to be robust. The main point to be highlighted here is that there is



449 indeed a qualitative difference in particles present in the three wetness categories, as averaged and shown
450 in Figure 3a, which generally supports the effort to segregate these samples.

451

452

453 Further evidence that there is a qualitative difference in the three wetness categories is shown
454 using molecular genetic analysis (Figs. 3b, c). The analysis of fungal DNA sequences from 21 of the high
455 volume samples found 406 operational taxonomic units (OTUs), belonging to different fungal classes and
456 phyla. When organized by wetness type it was observed that 106 of these occurred only on Rainy
457 samples, 148 of these occurred on Dry samples, and 37 on Other samples, with some fraction occurring in
458 overlaps of each (Fig. 3c). This shows that the number of OTUs observed uniquely in either the Rainy or
459 Dry periods is greater than the number of OTUs present in both wetness types, suggesting that the fungal
460 communities in each grouping are relatively distinct. Further, Figure 3b shows a break-down of fungal
461 taxonomic groupings for each wetness group. This analysis shows that there is a qualitative difference in
462 taxonomic break-down between periods of Rainy and Dry. Specifically, during Dry periods there is an
463 increased fraction of Pucciniomycetes (green bar, Fig. 3c), Chytridiomycota (yellow), Sordariomycetes
464 (orange), and Eurotiomycetes (pink) when compared to the Rainy periods.

464

465

3.2 Atmospheric mass concentration of arabitol, mannitol, and fungal spores

466

467

468

469

470

471

472

473

474

475

476

477

478

479

480

481

482

483

484

485

486

487

488

489

490

491

492

493

494

495

496

497

498

499

To estimate fungal spore emission to the atmosphere, the concentration of arabitol and mannitol (Fig. 5a, b, Table S2) in each aerosol sample was averaged for all samples in each of the three wetness categories. The average TSP concentration of arabitol collected on Dry samples increased by a factor of 3.3 on Rainy samples ($35.2 \pm 10.5 \text{ ng m}^{-3}$), and the average TSP mannitol concentration on Rainy samples was higher by a factor of 3.7 ($44.9 \pm 13.8 \text{ ng m}^{-3}$). Figures 5a, b show the concentration variability for each wetness category, observed as the standard deviation from the distribution of individual samples. For each polyol, there is no overlap in the ranges shown, including the outliers of the Rainy and Dry category, suggesting a definitive and conceptually distinct separation between dry periods and those influenced by rain. The concentrations observed during Other periods is between those of the Dry and Rainy averages, as expected, given the difficulty in confidently assigning these uniquely to one of these categories. The observations here are roughly consistent with previous reports of polyol concentration, despite differences in local fungal communities and concentrations. For example, Rathnayake et al. (2016) observed 30.2 ng m^{-3} arabitol and 41.3 ng m^{-3} mannitol in PM_{10} samples collected in rural Iowa, USA. In addition, Zhang et al. (2015) reported arabitol and mannitol concentrations in PM_{10} samples of 44.0 and 71.0 ng m^{-3} , respectively, from a study in the mountains on Hainan Island off the coast of Southern China.

The square of the correlation coefficient (R^2) here between concentration values of arabitol and mannitol during Rainy samples is very high (0.839; Table 1) suggesting that arabitol and mannitol originated from a primarily from the same source, likely active-discharge fungal spores. The correlation is similar to the $0.87 R^2$ reported by Bauer et al. (2008a) and the $0.93 R^2$ reported by Graham et al. (2003). In contrast, the same correlation between mannitol and arabitol concentrations, but for Dry samples is relatively low (0.312). This is consistent with reports that arabitol can be used more specifically as a spore tracer, but that mannitol has additional atmospheric sources besides fungal spores. The same correlation was also performed between arabitol or mannitol and other molecular tracers (endotoxins and (1 \rightarrow 3)- β -D-glucan), but all R^2 value were less than 0.43, suggesting that the endotoxins and glucans analyzed were not emitted uniquely from the same sources as arabitol and mannitol.

Results from the two UV-LIF instruments were averaged over high volume sample periods, and a correlation analysis was performed between tracer mass and fluorescent particle mass showing positive correlations in all cases. The FAP mass from the UV-APS shows high correlation with the fungal polyols during Rainy periods, with R^2 of 0.732 and 0.877 for arabitol and mannitol, respectively (Table 2; Figure 5c, d). The same tracers correlate poorly with the UV-LIF during Dry conditions. This is expected, because polyols such as arabitol and mannitol are only found in *Ascomycota* and *Basidiomycota* fungal spores which both utilize wet discharge methods for spore dispersal (Elbert et al., 2007; Feofilova, 2001;



500 Lewis and Smith, 1967). This high correlation suggests that the UV-APS does a good job of detecting
501 these wet-discharge spores, and corroborates previous statements that particles detected are often
502 predominately fungal spores (Healy et al., 2014; Huffman et al., 2013; Huffman et al., 2012). In contrast,
503 the low slope value and the poor correlation during Dry periods suggest that the UV-APS is also sensitive
504 to other kinds of particles, as designed. The small positive x-offset (FAP mass; Table S2, Figs. 5c,d)
505 during Rainy periods is likely due to particles that are too weakly fluorescent to be detected and counted
506 by the UV-APS, which is consistent with observations made in Brazil (Huffman et al., 2012).

507

508 Particle mass from WBS C11, assigned to fungal spores (Crawford et al., 2015), also correlated
509 strongly with the same two molecular tracers. Both Rainy periods (R^2 0.824) and Dry periods (R^2 0.764)
510 correlate well with arabitol (Fig. 5e), while mannitol (Fig. 5f) only shows a strong correlation during the
511 Rainy periods (R^2 0.799). Mannitol is a common polyol in higher plants while arabitol is only found in
512 fungal spores and lichen (Lewis and Smith, 1967). So the strong correlation of each polyol with UV-LIF
513 mass during Rainy periods when actively-discharged spores are expected to dominate and the similarly
514 strong correlations associated with arabitol suggests that the C11 cluster does a reasonably good job of
515 selecting fungal spore particles. The poor correlation between mannitol and C11 during dry periods
516 illustrates that the background mannitol concentration is likely not due to fungal spores alone, but has
517 contribution from other higher plants that contain mannitol. Particle concentrations detected by individual
518 WBS channels and in the other cluster were also compared with polyol concentrations, but each
519 correlation is relatively poor compared to that with respect to C11. As seen in Table 2 and Figures S2-S3,
520 correlations in FL1, 2, and 3 with arabitol are poor (<0.4) in the Dry category and good ($0.4 < R^2 < 0.7$) in
521 the Rainy category. For mannitol, all the UV-LIF instruments show high correlation (>0.7) in all cases.
522 This is likely due to mannitol being a non-specific tracer and suggests that the majority of UV-LIF
523 particles observed during all periods was dominated by PBAP.

524

525 3.3 Estimated number concentration of fungal spore aerosol

526 Bauer et al. (2008a) reported measurements of fungal spore number concentration in Vienna,
527 Austria using epifluorescence microscopy and also measured fungal tracer mass concentrations in order to
528 estimate the mass of arabitol (1.2 to 2.4 pg spore⁻¹) and mannitol (0.8 to 1.8 pg spore⁻¹) associated with
529 each emitted spore. Bauer et al. (2008a) and (Yttri et al., 2011b) reported ratios of mannitol to arabitol of
530 approximately 1.5 (\pm standard deviation of 26%) and 1.4 ± 0.3 , respectively. Our measurements show
531 slightly lower ratios of mannitol to arabitol, but that the ratio is dependent on wetness category; Rainy,
532 1.29 ± 0.17 ; Dry, 1.12 ± 0.23 ; and Other, 1.24 ± 0.54 . The mannitol to arabitol ratio would be expected to
533 vary as a function of fungal population present in the aerosol, whether between different wetness periods
534 at a given location or between different physical localities.

535

536 Using the approximate mid-point of the Bauer et al. (2008a) reported ranges, 1.7 pg mannitol per
537 spore and 1.2 pg arabitol per spore, atmospheric number concentrations of spores collected onto the high
538 volume filters were calculated from the polyol mass concentrations measured here. Based on these values,
539 and assuming all polyol mass originated with spore release, the mass concentration averages (Fig. 5) were
540 converted to fungal spore number concentrations (Fig. 6). The trends of spore concentration averages are
541 the same as with the polyol mass, because the numbers were each multiplied by the same scalar value.
542 After doing so, the analysis reveals an estimated spore concentration during Dry periods of 0.89×10^4 (\pm
543 0.21) spores m⁻³ using the arabitol concentration and 0.70×10^4 (± 0.19) spores m⁻³ using the mannitol
544 concentration (Table 3). The estimated concentration of spores increased approximately three-fold during
545 Rainy periods to 2.9×10^4 (± 0.8) spores m⁻³ (arabitol estimate) and 2.6×10^4 (± 0.8) spores m⁻³ (mannitol
546 estimate) (Figure 6a, b). These estimates match well with estimates reported by Spracklen and Heald
547 (2014), who modeled the concentration of airborne fungal spores across the globe as an average of $2.5 \times$
548 10^4 spores m⁻³, with approximately 0.5×10^4 spores m⁻³ over Colorado.

549



550 The UV-LIF instruments discussed here are fundamentally number-counting techniques and can
551 be utilized here roughly as spore counters. As a first approximation, each particle detected by the UV-
552 APS was assumed to be a fungal spore with the same properties used in the assumptions by Bauer et al.
553 (2008a). Plotting the correlation of fungal spore number concentration from polyol mass concentration
554 with respect to the fungal spore concentration assumed from the UV-LIF measurements shows
555 correlations in Figures 6c-f. The first, and most important observation is that the estimated fungal spore
556 concentration from each technique is on the same order of magnitude, 10^4 m^{-3} . Looking at individual
557 correlations reveals a finer layer of details. These results show that the number concentration of fungal
558 spores estimated by the UV-APS is greater than the number of fungal spores estimated by the tracers, as
559 evidenced by slope values of approximately 0.2 and 0.35 for Rainy and Dry conditions, respectively
560 (Figure 6c, d). The R^2 values (~ 0.5) during Rainy periods indicate that the additional source of particles
561 detected by the UV-APS is likely to have a similar source, such as PBAP mechanically ejected from soil
562 and vegetative surfaces with rain-splash (Huffman et al., 2013). The magnitude of the over-estimation is
563 higher during Dry periods, which would be expected if Rainy periods exhibited much higher particle
564 number fractions associated with polyol-containing spores.

565
566 The C11 cluster from WIBS data shows correlations with estimated fungal spores from arabinol
567 and mannitol that have slope much closer to 1.0 than correlations with UV-APS number (Figure 6e, f,
568 Table S3). For example, the slope of the C11 correlations with each polyol during Rainy periods is
569 approximately 0.87. This suggests only a 13% difference between the spore concentration estimates from
570 the two techniques during Rainy periods. The average number concentration of C11 during Rainy periods
571 is $1.6 \times 10^4 (\pm 0.8) \text{ spores m}^{-3}$. In both cases the slopes with respect to C11 is greater than 1.0 during Dry
572 periods, suggesting that the cluster method may be missing some fraction of weakly fluorescent particles.
573 Huffman et al. (2012) similarly suggests that that particles that are weakly fluorescent may be below the
574 detection limit of the instrument, and Healy et al. (2014) suggested that both UV-APS and WIBS-4
575 instruments significantly under-count the ubiquitous *Cladosporium* spores that are most common during
576 dry weather and often peak in the afternoon when RH is low (De Groot, 1968; Oliveira et al., 2009).
577 Fundamentally, however, the results from the UV-APS, and even more so the numbers reported by the
578 clustering analysis by Crawford et al. (2015), reveal broadly similar trends with the numbers estimated
579 from polyol-to-spore values reported by Bauer et al. (2008a).

580
581 The fungal culture samples show similar division during Rainy and Dry periods as arabinol and
582 mannitol concentrations (Figure 6c), with an increase of approx. 1.6 during Rainy periods. The trend of a
583 positive slope with respect to the UV-LIF measurements is also similar between the tracer and culturing
584 methods. In general, however, the R^2 value correlating CFU to fungal spore number calculated from UV-
585 LIF number is lower than between tracers and UV-LIF numbers (Tables 2, S4). This is not unexpected for
586 several reasons. First, the short sampling time of the culture samples (20 min) leads to poor counting
587 statistics and high number concentration variability, whereas each data point from the high volume air
588 samples represents a period of 4 – 48 hours. Second, culture samplers, by their nature, only account for
589 cultural fungal spores. It has been estimated that as low as 17% of aerosolized fungal spores are
590 culturable, and so it is expected that the CFU concentration observed is significantly less than the total
591 airborne concentration of spores (Bridge and Spooner, 2001; Després et al., 2012). Nonetheless, the
592 culturing analysis here supports the tracer and UV-LIF analyses and the most important trends are
593 consistent between all analysis methods. The concentration of fungal spores is higher during the Rainy
594 periods, and there is a positive correlation between both tracer and CFU concentration and UV-LIF
595 number.

596
597 In pristine environment, such as the Amazon, supermicron particle mass has been found to consist
598 of up to 85% biological material (Pöschl et al., 2010). Total particulate matter mass was calculated here
599 from the UV-APS number concentrations (m^{-3}) and converted to mass for particles of aerodynamic
600 diameter 0.5 – 15 μm . In only this case a density of 1.5 g cm^{-3} was utilized to calculate a first



601 approximation of total particle mass to which all other mass measurements were compared. An average
602 TSP mass density of 1.5 g cm^{-3} was utilized, because organic aerosol is typically estimated with density $<$
603 1.0 g cm^{-3} , biological particles are often assumed to have ca. 1.0 g cm^{-3} density, and mineral dust
604 particles have densities of up to ca. 3.5 g cm^{-3} (Dexter, 2004; Tegen and Fung, 1994). Fungal spore mass
605 was estimated here using the fungal spore concentrations calculated from arabitol and mannitol mass (Fig.
606 6) and then using an estimated 33 pg reported by Bauer et al. (2008b) as an average mass per spore.
607 Dividing the resultant fungal spore mass by total particulate mass provides a relative mass fraction for
608 each high volume sample period. These calculations suggest that fungal spores represent approximately
609 $23\% \pm 9$ (using arabitol) or $21\% \pm 8$ (using mannitol) of total particulate mass during Rainy periods
610 (Table 3, Figure 7). This represents a nearly 6 fold increase in percentage compared to Dry periods (4.8%
611 ± 1.4 and $3.7\% \pm 1.1$, respectively). A similar increase during Rainy periods was also seen in the mass
612 fraction of fungal cluster C11, which represented $17\% \pm 10$ of the particle mass during Rainy and $2\% \pm 1$
613 during Dry periods (Table S4).

614

615 3.5 Variations in endotoxin and glucan concentrations

616 Endotoxins are components of gram-negative bacteria (Andreae and Crutzen, 1997). Here, we
617 show correlations between total endotoxin mass and WBS Cl_{Bact} , which were assigned by Crawford et al.
618 (2015) to be bacteria due to the small particle size ($< 1 \mu\text{m}$) and high correlation with rain. These cluster
619 assignments are quite uncertain, however, and should be treated loosely. The correlation between
620 endotoxin mass and UV-APS and the WBS clusters was very poor, in most cases $R^2 < 0.1$ (Table 2,
621 Figure 8), suggesting no apparent relationship. Analysis of bacteria by both UV-LIF techniques is
622 hampered by the fact that bacteria can be $< 1 \mu\text{m}$ in size and because both instruments detect particles
623 with decreased efficiency at sizes below $0.8 \mu\text{m}$. So weak correlations may not have been apparent due to
624 reduced overlap in particle size. Despite the lack of apparent correlation between the techniques, the
625 relatively variable endotoxin concentrations were elevated during Rainy periods, consistent with Jones
626 and Harrison (2004), who showed that bacteria concentration were elevated after rainy periods.

627 Glucans, such as (1 \rightarrow 3)- β -D-glucan, are components of the cell walls of pollen, fungal spores,
628 plant detritus, and bacteria (Chow et al., 2015b; Lee et al., 2006; Stone and Clarke, 1992). In contrast to
629 the observed difference in endotoxin concentration during the different wetness periods, however, (1 \rightarrow 3)-
630 β -D-glucan showed no correlations with UV-LIF concentrations (Table 2) and no differentiation during
631 the different wetness periods.

632

633 4. Conclusions

634 Increased concentrations of fluorescent aerosol particles and ice nuclei attributed to having
635 biological origin were observed during and immediately after rain events throughout the BEACHON-
636 RoMBAS study in 2011 (Huffman et al., 2013; Prenni et al., 2013; Schumacher et al., 2013). Here we
637 expand upon the previous reports by utilizing measurements from two commercially available UV-LIF
638 instruments, of several molecular tracers extracted from high volume filter samples, and from a culture-
639 based sampler in order to compare three very different methods of atmospheric fungal spore analysis.
640 This study represents the first reported correlation of UV-LIF and molecular tracer measurements and
641 provided an opportunity to understand how an important class of PBAP might be influenced by periods of
642 rainy and dry weather. We found clear patterns in the fungal molecular tracers, arabitol and mannitol,
643 associated with Rainy conditions that are consistent with previous findings (Bauer et al., 2008a; Elbert et
644 al., 2007; Feofilova, 2001). Fungal polyols increased 3-fold over Dry conditions during Rainy weather
645 samples, with arabitol concentration of $35.2 \pm 10.5 \text{ ng m}^{-3}$ and mannitol concentration of $44.9 \pm 13.8 \text{ ng}$
646 m^{-3} . Additionally, the very high correlation of the fungal tracers with WBS C11 ($R^2 > 0.8$ in many cases)
647 provides support for its assignment by Crawford et al. (2015) to fungal spores. Similarly, the UV-APS
648 correlates well with fungal tracers, however over-counts the number concentration estimated from the
649 tracers, confirming that the UV-APS is sensitive also to other types of particles beyond fungal spores, as
650 expected. The estimated spore count from the WBS C11 concentration was within $\sim 13\%$ of the spore
651 count estimated by the tracer method, with concentrations ranging from $1.6 - 2.9 \times 10^4 \text{ spores m}^{-3}$. These



652 values are broadly consistent with concentrations modeled by, e.g. Spracklen and Heald (2014), Hoose et
653 al. (2010), and Hummel et al. (2015). These spore counts represent 17-23% of the total particle mass
654 during Rainy conditions and 2-4% during Dry conditions. Culture-based sampling also shows a similar
655 relationship between CFU and UV-LIF concentrations and an increase of ~1.6 between Dry and Rainy
656 conditions. Despite the fact that the tracer and UV-LIF approaches to estimating atmospheric fungal spore
657 concentration are fundamentally different, they provide remarkably similar estimates and temporal trends.
658 With further improvements in instrumentation and analysis methods (e.g. advanced clustering algorithms
659 applied to UV-LIF data), the ability to reliably discriminate between PBAP types is improving. As we
660 have shown here, this technology represents a potential for monitoring approximate fungal spore mass
661 and for contributing improved information on fungal spore concentration to global and regional models
662 that to this point has been lacking (Spracklen and Heald, 2014).

663

664

665 5. Acknowledgements

666 The BEACHON-RoMBAS campaign was partially supported by an ETBC (Emerging Topics in
667 Biogeochemical Cycles) grant to the National Center for Atmospheric Research (NCAR), the University
668 of Colorado, Colorado State University, and Penn State University (NSF ATM-0919189). The authors
669 wish to thank Jose Jimenez, Douglas Day (Univ. Colorado-Boulder); Anthony Prenni, Paul DeMott,
670 Sonia Kreidenweis, and Jessica Prenni (Colorado St. Univ.); Alex Guenther, and Jim Smith (NCAR) for
671 BEACHON-RoMBAS project organization and logistical support and the USFS, NCAR, and Richard
672 Oakes for access to the Manitou Experimental Forest Observatory field site. Measurements of
673 temperature, relative humidity, wind speed, and wind direction were provided by Andrew Turnipseed
674 (NCAR) and leaf wetness and disdrometer data were provided by Dave Gochis (NCAR). Marie I.
675 Gosselin thanks the Max Planck Society for financial support. J. Alex Huffman thanks the University of
676 Denver for intramural funding for faculty support. The Mainz team acknowledges financial support from
677 the Max Planck Society (MPG), the Max Planck Graduate Center with the Johannes Gutenberg
678 University Mainz (MPGC), the Geocycles Cluster Mainz (LEC Rheinland-Pfalz), and the German
679 Research Foundation (DFG PO1013/5-1 and FR3641/1-2, FOR 1525 INUIT). The Manchester team
680 acknowledges funding from the UK NERC (UK-BEACHON, Grant # NE/H019049/1) to participate in
681 the BEACHON experiment, and development support of the WIBS instruments. Manchester would also
682 like to thank Prof. Paul Kaye, the developer of the WIBS instruments and his team at the University of
683 Hertfordshire, for their technical support. The authors thank Cristina Ruzene, Isabell Müller-Germann,
684 Petya Yordanova, Tobias Könemann (Max Planck Inst. For Chem.), and Nicole Savage (Univ. Denver)
685 for technical assistance.



686 **6. References**

687

688 Allitt, U.: Airborne fungal spores and the thunderstorm of 24 June 1994, *Aerobiologia*, 16, 397-406,
689 2000.

690 Andreae, M. O. and Crutzen, P. J.: Atmospheric Aerosols: Biogeochemical Sources and Role in
691 Atmospheric Chemistry, *Science*, 276, 1052-1058, 1997.

692 Axelsson, B.-O., Saraf, A., and Larsson, L.: Determination of ergosterol in organic dust by gas
693 chromatography-mass spectrometry, *Journal of Chromatography B: Biomedical Sciences and*
694 *Applications*, 666, 77-84, 1995.

695 Barbaro, E., Kirchgeorg, T., Zangrando, R., Vecchiato, M., Piazza, R., Barbante, C., and Gambaro, A.:
696 Sugars in Antarctic aerosol, *Atmos Environ*, 118, 135-144, 2015.

697 Bauer, H., Claeys, M., Vermeylen, R., Schueller, E., Weinke, G., Berger, A., and Puxbaum, H.: Arabitol
698 and mannitol as tracers for the quantification of airborne fungal spores, *Atmos Environ*, 42, 588-593,
699 2008a.

700 Bauer, H., Schueller, E., Weinke, G., Berger, A., Hitzemberger, R., Marr, I. L., and Puxbaum, H.:
701 Significant contributions of fungal spores to the organic carbon and to the aerosol mass balance of the
702 urban atmospheric aerosol, *Atmos Environ*, 42, 5542-5549, 2008b.

703 Bigg, E. K., Soubeyrand, S., and Morris, C. E.: Persistent after-effects of heavy rain on concentrations of
704 ice nuclei and rainfall suggest a biological cause, *Atmos Chem Phys*, 15, 2313-2326, 2015.

705 Bridge, P. and Spooner, B.: Soil fungi: diversity and detection, *Plant and soil*, 232, 147-154, 2001.

706 Buller, A.: Spore deposits—the number of spores, *Researches on fungi*, 1, 79-88, 1909.

707 Burger, H.: Official Publication of American Academy of Allergy and Immunology: Bioaerosols:
708 Prevalence and health effects in the indoor environment, *Journal of Allergy and Clinical Immunology*, 86,
709 687-701, 1990.

710 Burshtein, N., Lang-Yona, N., and Rudich, Y.: Ergosterol, arabitol and mannitol as tracers for biogenic
711 aerosols in the eastern Mediterranean, *Atmos Chem Phys*, 11, 829-839, 2011.

712 Caseiro, A., Marr, I. L., Claeys, M., Kasper-Giebl, A., Puxbaum, H., and Pio, C. A.: Determination of
713 saccharides in atmospheric aerosol using anion-exchange high-performance liquid chromatography and
714 pulsed-amperometric detection, *Journal of Chromatography A*, 1171, 37-45, 2007.

715 Cheng, J. Y. W., Hui, E. L. C., and Lau, A. P. S.: Bioactive and total endotoxins in atmospheric aerosols
716 in the Pearl River Delta region, China, *Atmos Environ*, 47, 3-11, 2012.

717 Chow, J. C., Lowenthal, D. H., Chen, L.-W. A., Wang, X., and Watson, J. G.: Mass reconstruction
718 methods for PM_{2.5}: a review, *Air Quality, Atmosphere & Health*, 8, 243-263, 2015a.

719 Chow, J. C., Yang, X., Wang, X., Kohl, S. D., Hurbain, P. R., Chen, L. A., and Watson, J. G.:
720 Characterization of Ambient PM₁₀ Bioaerosols in a California Agricultural Town, *Aerosol Air Qual Res*,
721 15, 1433-1447, 2015b.



- 722 Crawford, I., Robinson, N. H., Flynn, M. J., Foot, V. E., Gallagher, M. W., Huffman, J. A., Stanley, W.
723 R., and Kaye, P. H.: Characterisation of bioaerosol emissions from a Colorado pine forest: results from
724 the BEACHON-RoMBAS experiment, *Atmos Chem Phys*, 14, 8559-8578, 2014.
- 725 Crawford, I., Ruske, S., Topping, D., and Gallagher, M.: Evaluation of hierarchical agglomerative cluster
726 analysis methods for discrimination of primary biological aerosol, *Atmos Meas Tech*, 8, 4979-4991,
727 2015.
- 728 Dales, R. E., Cakmak, S., Judek, S., Dann, T., Coates, F., Brook, J. R., and Burnett, R. T.: The role of
729 fungal spores in thunderstorm asthma, *Chest*, 123, 745-750, 2003.
- 730 De Groot, R.: Diurnal cycles of air-borne spores produced by forest fungi, *Phytopathology*, 58, 1223-
731 1229, 1968.
- 732 Deguillaume, L., Leriche, M., Amato, P., Ariya, P. A., Delort, A. M., Pöschl, U., Chaumerliac, N., Bauer,
733 H., Flossmann, A. I., and Morris, C. E.: Microbiology and atmospheric processes: chemical interactions
734 of primary biological aerosols, *Biogeosciences*, 5, 1073-1084, 2008.
- 735 Després, V. R., Huffman, J. A., Burrows, S. M., Hoose, C., Safatov, A. S., Buryak, G., Frohlich-
736 Nowoisky, J., Elbert, W., Andreae, M. O., Poschl, U., and Jaenicke, R.: Primary biological aerosol
737 particles in the atmosphere: a review, *Tellus B*, 64, 58, 2012.
- 738 Dexter, A.: Soil physical quality: Part I. Theory, effects of soil texture, density, and organic matter, and
739 effects on root growth, *Geoderma*, 120, 201-214, 2004.
- 740 Di Filippo, P., Pomata, D., Riccardi, C., Buiarelli, F., and Perrino, C.: Fungal contribution to size-
741 segregated aerosol measured through biomarkers, *Atmos Environ*, 64, 132-140, 2013.
- 742 Douwes, J., Thorne, P., Pearce, N., and Heederik, D.: Bioaerosol health effects and exposure assessment:
743 progress and prospects, *Annals of Occupational Hygiene*, 47, 187-200, 2003.
- 744 Elbert, W., Taylor, P. E., Andreae, M. O., and Poschl, U.: Contribution of fungi to primary biogenic
745 aerosols in the atmosphere: wet and dry discharged spores, carbohydrates, and inorganic ions, *Atmos
746 Chem Phys*, 7, 4569-4588, 2007.
- 747 Faulwetter, R.: Wind-blown rain, a factor in disease dissemination, *J. agric. Res*, 10, 639-648, 1917.
- 748 Feofilova, E. P.: The Kingdom Fungi: Heterogeneity of Physiological and Biochemical Properties and
749 Relationships with Plants, Animals, and Prokaryotes (Review), *Applied Biochemistry and Microbiology*,
750 37, 124-137, 2001.
- 751 Foot, V. E., Kaye, P. H., Stanley, W. R., Barrington, S. J., Gallagher, M., and Gabey, A.: Low-cost real-
752 time multiparameter bio-aerosol sensors, 2008, 71160I-71160I-71112.
- 753 Frankland, A. and Gregory, P.: Allergenic and agricultural implications of airborne ascospore
754 concentrations from a fungus, *Didymella exitialis*, 1973. 1973.
- 755 Fröhlich-Nowoisky, J., Burrows, S., Xie, Z., Engling, G., Solomon, P., Fraser, M., Mayol-Bracero, O.,
756 Artaxo, P., Begerow, D., and Conrad, R.: Biogeography in the air: fungal diversity over land and oceans,
757 *Biogeosciences*, 9, 1125-1136, 2012.



- 758 Fröhlich-Nowoisky, J., Kampf, C. J., Weber, B., Huffman, J. A., Pöhlker, C., Andreae, M. O., Lang-
759 Yona, N., Burrows, S. M., Gunthe, S. S., Elbert, W., Su, H., Hoor, P., Thines, E., Hoffmann, T., Després,
760 V. R., and Pöschl, U.: Bioaerosols in the Earth system: Climate, health, and ecosystem interactions,
761 Atmospheric Research, 182, 346-376, doi: 10.1016/j.atmosres.2016.07.018, 2016.
- 762 Fröhlich-Nowoisky, J., Pickersgill, D. A., Després, V. R., and Pöschl, U.: High diversity of fungi in air
763 particulate matter, Proceedings of the National Academy of Sciences, 106, 12814-12819, 2009.
- 764 Gabey, A., Gallagher, M., Whitehead, J., Dorsey, J., Kaye, P. H., and Stanley, W.: Measurements and
765 comparison of primary biological aerosol above and below a tropical forest canopy using a dual channel
766 fluorescence spectrometer, Atmos Chem Phys, 10, 4453-4466, 2010.
- 767 Gilardoni, S., Vignati, E., Marmer, E., Cavalli, F., Belis, C., Gianelle, V., Loureiro, A., and Artaxo, P.:
768 Sources of carbonaceous aerosol in the Amazon basin, Atmos Chem Phys, 11, 2747-2764, 2011.
- 769 Gonçalves, F. L. T., Bauer, H., Cardoso, M. R. A., Pukinskaskas, S., Matos, D., Melhem, M., and Puxbaum,
770 H.: Indoor and outdoor atmospheric fungal spores in the São Paulo metropolitan area (Brazil): species and
771 numeric concentrations, International journal of biometeorology, 54, 347-355, 2010.
- 772 Graham, B., Guyon, P., Taylor, P. E., Artaxo, P., Maenhaut, W., Glovsky, M. M., Flagan, R. C., and
773 Andreae, M. O.: Organic compounds present in the natural Amazonian aerosol: Characterization by gas
774 chromatography-mass spectrometry, J Geophys Res-Atmos, 108, 4766-4766, 2003.
- 775 Gregory, P. H. and Sreeramulu, T.: Air spora of an estuary, T Brit Mycol Soc, 41, 145-156, 1958.
- 776 Haga, D., Iannone, R., Wheeler, M., Mason, R., Polishchuk, E., Fetch, T., Kamp, B., McKendry, I., and
777 Bertram, A.: Ice nucleation properties of rust and bunt fungal spores and their transport to high altitudes,
778 where they can cause heterogeneous freezing, Journal of Geophysical Research: Atmospheres, 118, 7260-
779 7272, 2013.
- 780 Hairston, P. P., Ho, J., and Quant, F. R.: Design of an instrument for real-time detection of bioaerosols
781 using simultaneous measurement of particle aerodynamic size and intrinsic fluorescence, Journal of
782 Aerosol Science, 28, 471-482, 1997.
- 783 Heald, C. L. and Spracklen, D. V.: Atmospheric budget of primary biological aerosol particles from
784 fungal spores, Geophysical Research Letters, 36, L09806/09801-L09806/09805, 2009.
- 785 Healy, D., Huffman, J., O'Connor, D., Pöhlker, C., Pöschl, U., and Sodeau, J.: Ambient measurements of
786 biological aerosol particles near Killarney, Ireland: a comparison between real-time fluorescence and
787 microscopy techniques, Atmos Chem Phys, 14, 8055-8069, 2014.
- 788 Hernandez, M., Perring, A. E., McCabe, K., Kok, G., Granger, G., and Baumgardner, D.: Chamber
789 catalogues of optical and fluorescent signatures distinguish bioaerosol classes, Atmos Meas Tech, 9,
790 3283-3292, 2016.
- 791 Hill, S. C., Mayo, M. W., and Chang, R. K.: Fluorescence of bacteria, pollens, and naturally occurring
792 airborne particles: excitation/emission spectra, DTIC Document, 2009.
- 793 Hirst, J. and Stedman, O.: Dry liberation of fungus spores by raindrops, Microbiology, 33, 335-344, 1963.



- 794 Hoose, C., Kristjánsson, J. E., Chen, J.-P., and Hazra, A.: A Classical-Theory-Based Parameterization of
795 Heterogeneous Ice Nucleation by Mineral Dust, Soot, and Biological Particles in a Global Climate Model,
796 *Journal of the Atmospheric Sciences*, 67, 2483-2503, 2010.
- 797 Huffman, J. A., Prenni, A. J., DeMott, P. J., Pöhlker, C., Mason, R. H., Robinson, N. H., Fröhlich-
798 Nowoisky, J., Tobo, Y., Després, V. R., Garcia, E., Gochis, D. J., Harris, E., Müller-Germann, I., Ruzene,
799 C., Schmer, B., Sinha, B., Day, D. A., Andreae, M. O., Jimenez, J. L., Gallagher, M., Kreidenweis, S. M.,
800 Bertram, A. K., and Pöschl, U.: High concentrations of biological aerosol particles and ice nuclei during
801 and after rain, *Atmos. Chem. Phys.*, 13, 6151-6164, 2013.
- 802 Huffman, J. A. and Santarpia, J.: Online techniques for quantification and characterization of biological
803 aerosol. In: *Microbiology of aerosols*, Delort, A.-M. and Amato, P. (Eds.), Wiley, Hoboken, NJ, 2016.
- 804 Huffman, J. A., Sinha, B., Garland, R. M., Snee-Pollmann, A., Gunthe, S. S., Artaxo, P., Martin, S. T.,
805 Andreae, M. O., and Pöschl, U.: Size distributions and temporal variations of biological aerosol particles
806 in the Amazon rainforest characterized by microscopy and real-time UV-APS fluorescence techniques
807 during AMAZE-08, *Atmos. Chem. Phys.*, 12, 11997-12019, 2012.
- 808 Hummel, M., Hoose, C., Gallagher, M., Healy, D. A., Huffman, J. A., O'Connor, D., Poeschl, U.,
809 Poehlker, C., Robinson, N. H., Schnaiter, M., Sodeau, J. R., Stengel, M., Toprak, E., and Vogel, H.:
810 Regional-scale simulations of fungal spore aerosols using an emission parameterization adapted to local
811 measurements of fluorescent biological aerosol particles, *Atmos Chem Phys*, 15, 6127-6146, 2015.
- 812 Ingold, C. T.: Fungal spores. Their liberation and dispersal, *Fungal spores. Their liberation and dispersal.*,
813 1971. 1971.
- 814 Jones, A. M. and Harrison, R. M.: The effects of meteorological factors on atmospheric bioaerosol
815 concentrations—a review, *Science of the Total Environment*, 326, 151-180, 2004.
- 816 Kaye, P., Stanley, W., Hirst, E., Foot, E., Baxter, K., and Barrington, S.: Single particle multichannel bio-
817 aerosol fluorescence sensor, *Optics Express*, 13, 3583-3593, 2005.
- 818 Lau, A. P. S., Lee, A. K. Y., Chan, C. K., and Fang, M.: Ergosterol as a biomarker for the quantification
819 of the fungal biomass in atmospheric aerosols, *Atmos Environ*, 40, 249-259, 2006.
- 820 Laumbach, R. J. and Kipen, H. M.: Bioaerosols and sick building syndrome: particles, inflammation, and
821 allergy, *Current opinion in allergy and clinical immunology*, 5, 135-139, 2005.
- 822 Lee, T., Grinshpun, S. A., Kim, K. Y., Iossifova, Y., Adhikari, A., and Reponen, T.: Relationship between
823 indoor and outdoor airborne fungal spores, pollen, and (1→3)-β-D-glucan in homes without visible mold
824 growth, *Aerobiologia*, 22, 227-235, 2006.
- 825 Lee, T., Sullivan, A. P., Mack, L., Jimenez, J. L., Kreidenweis, S. M., Onasch, T. B., Worsnop, D. R.,
826 Malm, W., Wold, C. E., Hao, W. M., and Collett, J. L., Jr.: Chemical Smoke Marker Emissions During
827 Flaming and Smoldering Phases of Laboratory Open Burning of Wildland Fuels, *Aerosol Science and*
828 *Technology*, 44, I-V, 2010.
- 829 Lewis, D. H. and Smith, D. C.: Sugar alcohols (polyols) in fungi and green plants, *New Phytol*, 66, 185-
830 204, 1967.



- 831 Liang, L., Engling, G., He, K., Du, Z., Cheng, Y., and Duan, F.: Evaluation of fungal spore characteristics
832 in Beijing, China, based on molecular tracer measurements, *Environmental Research Letters*, 8, 014005,
833 2013.
- 834 Lin, W.-H. and Li, C.-S.: Associations of fungal aerosols, air pollutants, and meteorological factors,
835 *Aerosol Science & Technology*, 32, 359-368, 2000.
- 836 Madden, L.: Effects of rain on splash dispersal of fungal pathogens, *Canadian Journal of Plant Pathology*,
837 19, 225-230, 1997.
- 838 Madelin, T.: Fungal aerosols: a review, *Journal of Aerosol Science*, 25, 1405-1412, 1994.
- 839 Miller, J. D. and Young, J. C.: The use of ergosterol to measure exposure to fungal propagules in indoor
840 air, *American Industrial Hygiene Association Journal*, 58, 39-43, 1997.
- 841 Morris, C., Sands, D., Glaux, C., Samsatly, J., Asaad, S., Moukahel, A., Goncalves, F. L. T., and Bigg, E.:
842 Urediospores of rust fungi are ice nucleation active at >-10 C and harbor ice nucleation active bacteria,
843 *Atmos Chem Phys*, 13, 4223-4233, 2013.
- 844 Oliveira, M., Ribeiro, H., Delgado, J., and Abreu, I.: The effects of meteorological factors on airborne
845 fungal spore concentration in two areas differing in urbanisation level, *International journal of*
846 *biometeorology*, 53, 61-73, 2009.
- 847 Ortega, J., Turnipseed, A., Guenther, A. B., Karl, T. G., Day, D. A., Gochis, D., Huffman, J. A., Prenni,
848 A. J., Levin, E. J. T., Kreidenweis, S. M., DeMott, P. J., Tobo, Y., Patton, E. G., Hodzic, A., Cui, Y. Y.,
849 Harley, P. C., Hornbrook, R. S., Apel, E. C., Monson, R. K., Eller, A. S. D., Greenberg, J. P., Barth, M.
850 C., Campuzano-Jost, P., Palm, B. B., Jimenez, J. L., Aiken, A. C., Dubey, M. K., Geron, C., Offenberg,
851 J., Ryan, M. G., Formwalt, P. J., Pryor, S. C., Keutsch, F. N., DiGangi, J. P., Chan, A. W. H., Goldstein,
852 A. H., Wolfe, G. M., Kim, S., Kaser, L., Schnitzhofer, R., Hansel, A., Cantrell, C. A., Mauldin, R. L., and
853 Smith, J. N.: Overview of the Manitou Experimental Forest Observatory: site description and selected
854 science results from 2008 to 2013, *Atmos Chem Phys*, 14, 6345-6367, 2014.
- 855 Perring, A., Schwarz, J., Baumgardner, D., Hernandez, M., Spracklen, D., Heald, C., Gao, R., Kok, G.,
856 McMeeking, G., and McQuaid, J.: Airborne observations of regional variation in fluorescent aerosol
857 across the United States, *Journal of Geophysical Research: Atmospheres*, 120, 1153-1170, 2015.
- 858 Pöhlker, C., Huffman, J. A., Forster, J. D., and Pöschl, U.: Autofluorescence of atmospheric bioaerosols:
859 spectral fingerprints and taxonomic trends of pollen, *Atmos Meas Tech*, 6, 3369-3392, 2013.
- 860 Pöhlker, C., Huffman, J. A., and Pöschl, U.: Autofluorescence of atmospheric bioaerosols-fluorescent
861 biomolecules and potential interferences, *Atmos Meas Tech*, 5, 37-71, 2012a.
- 862 Pöhlker, C., Wiedemann, K. T., Sinha, B., Shiraiwa, M., Gunthe, S. S., Smith, M., Su, H., Artaxo, P.,
863 Chen, Q., and Cheng, Y.: Biogenic potassium salt particles as seeds for secondary organic aerosol in the
864 Amazon, *Science*, 337, 1075-1078, 2012b.
- 865 Pöschl, U., Martin, S., Sinha, B., Chen, Q., Gunthe, S., Huffman, J., Borrmann, S., Farmer, D., Garland,
866 R., and Helas, G.: Rainforest aerosols as biogenic nuclei of clouds and precipitation in the Amazon,
867 *Science*, 329, 1513-1516, 2010.



- 868 Pöschl, U. and Shiraiwa, M.: Multiphase chemistry at the atmosphere–biosphere interface influencing
869 climate and public health in the Anthropocene, *Chemical reviews*, 115, 4440-4475, 2015.
- 870 Prenni, A. J., Tobo, Y., Garcia, E., DeMott, P. J., Huffman, J. A., McCluskey, C. S., Kreidenweis, S. M.,
871 Prenni, J. E., Pöhlker, C., and Pöschl, U.: The impact of rain on ice nuclei populations at a forested site in
872 Colorado, *Geophysical Research Letters*, 40, 227-231, 2013.
- 873 Pyrri, I. and Kapsanaki-Gotsi, E.: A comparative study on the airborne fungi in Athens, Greece, by viable
874 and non-viable sampling methods, *Aerobiologia*, 23, 3-15, 2007.
- 875 Rasband, W. and ImageJ, U.: Bethesda, Md, USA. ImageJ, 1997.
- 876 Rathnayake, C. M., Metwali, N., Baker, Z., Jayarathne, T., Kostle, P. A., Thorne, P. S., O'Shaughnessy, P.
877 T., and Stone, E. A.: Urban enhancement of PM10 bioaerosol tracers relative to background locations in
878 the Midwestern United States, *Journal of Geophysical Research: Atmospheres*, 121, 5071-5089, 2016.
- 879 Robinson, N. H., Allan, J. D., Huffman, J. A., Kaye, P. H., Foot, V. E., and Gallagher, M.: Cluster
880 analysis of WIBS single-particle bioaerosol data, *Atmos Meas Tech*, 6, 337-347, 2013.
- 881 Saari, S., Niemi, J., Rönkkö, T., Kuuluvainen, H., Järvinen, A., Pirjola, L., Aurela, M., Hillamo, R., and
882 Keskinen, J.: Seasonal and diurnal variations of fluorescent bioaerosol concentration and size distribution
883 in the urban environment, *Aerosol and Air Quality Research*, 15, 572-581, 2015.
- 884 Saari, S., Putkiranta, M., and Keskinen, J.: Fluorescence spectroscopy of atmospherically relevant
885 bacterial and fungal spores and potential interferences, *Atmos Environ*, 71, 202-209, 2013.
- 886 Schauer, J. J., Rogge, W. F., Hildemann, L. M., Mazurek, M. A., Cass, G. R., and Simoneit, B. R. T.:
887 Source apportionment of airborne particulate matter using organic compounds as tracers, *Atmos Environ*,
888 30, 3837-3855, 1996.
- 889 Schumacher, C. J., Pöhlker, C., Aalto, P., Hiltunen, V., Petäjä, T., Kulmala, M., Pöschl, U., and Huffman,
890 J. A.: Seasonal cycles of fluorescent biological aerosol particles in boreal and semi-arid forests of Finland
891 and Colorado, *Atmos. Chem. Phys.*, 13, 11987-12001, 2013.
- 892 Sesartic, A. and Dallafior, T. N.: Global fungal spore emissions, review and synthesis of literature data,
893 *Biogeosciences*, 8, 1181-1192, 2011.
- 894 Sesartic, A., Lohmann, U., and Storelvmo, T.: Modelling the impact of fungal spore ice nuclei on clouds
895 and precipitation, *Environmental Research Letters*, 8, 014029, 2013.
- 896 Simoneit, B. R. and Mazurek, M.: Organic tracers in ambient aerosols and rain, *Aerosol Science and
897 Technology*, 10, 267-291, 1989.
- 898 Simoneit, B. R. T., Kobayashi, M., Mochida, M., Kawamura, K., Lee, M., Lim, H.-J., Turpin, B. J., and
899 Komazaki, Y.: Composition and major sources of organic compounds of aerosol particulate matter
900 sampled during the ACE-Asia campaign, *Journal of Geophysical Research*, [Atmospheres], 109,
901 D19S10/11-D19S10/22, 2004.
- 902 Sodeau, J. and O'Connor, D.: Bioaerosol Monitoring of the Atmosphere for Occupational and
903 Environmental Purposes, *Comprehensive Analytical Chemistry*, 2016. 2016.



- 904 Spracklen, D. and Heald, C. L.: The contribution of fungal spores and bacteria to regional and global
905 aerosol number and ice nucleation immersion freezing rates, *Atmos Chem Phys*, 14, 9051-9059, 2014.
- 906 Stone, B. and Clarke, A.: *Chemistry and biology of (1, 3)-D-glucans*, Victoria, Australia.: La Trobe
907 University Press, 1992. 236-239, 1992.
- 908 Taylor, P. E. and Jonsson, H.: Thunderstorm asthma, *Current allergy and asthma reports*, 4, 409-413,
909 2004.
- 910 Tegen, I. and Fung, I.: Modeling of mineral dust in the atmosphere: Sources, transport, and optical
911 thickness, *Journal of Geophysical Research: Atmospheres*, 99, 22897-22914, 1994.
- 912 Tobo, Y., Prenni, A. J., DeMott, P. J., Huffman, J. A., McCluskey, C. S., Tian, G., Pöhlker, C., Pöschl,
913 U., and Kreidenweis, S. M.: Biological aerosol particles as a key determinant of ice nuclei populations in
914 a forest ecosystem, *Journal of Geophysical Research: Atmospheres*, 118, 10,100-110,110, 2013.
- 915 Toprak, E. and Schnaiter, M.: Fluorescent biological aerosol particles measured with the Waveband
916 Integrated Bioaerosol Sensor WIBS-4: laboratory tests combined with a one year field study, *Atmos.*
917 *Chem. Phys.*, 13, 225-243, 2013.
- 918 Weete, J. D.: Sterols of the fungi: distribution and biosynthesis, *Phytochemistry*, 12, 1843-1864, 1973.
- 919 Womiloju, T. O., Miller, J. D., Mayer, P. M., and Brook, J. R.: Methods to determine the biological
920 composition of particulate matter collected from outdoor air, *Atmos Environ*, 37, 4335-4344, 2003.
- 921 Yang, Y., Chan, C.-y., Tao, J., Lin, M., Engling, G., Zhang, Z., Zhang, T., and Su, L.: Observation of
922 elevated fungal tracers due to biomass burning in the Sichuan Basin at Chengdu City, China, *Science of*
923 *the Total Environment*, 431, 68-77, 2012.
- 924 Yttri, K. E., Simpson, D., Noejgaard, J. K., Kristensen, K., Genberg, J., Stenstrom, K., Swietlicki, E.,
925 Hillamo, R., Aurela, M., Bauer, H., Offenberg, J. H., Jaoui, M., Dye, C., Eckhardt, S., Burkhardt, J. F.,
926 Stohl, A., and Glasius, M.: Source apportionment of the summer time carbonaceous aerosol at Nordic
927 rural background sites, *Atmos Chem Phys*, 11, 13339-13357, 2011a.
- 928 Yttri, K. E., Simpson, D., Stenstrom, K., Puxbaum, H., and Svendby, T.: Source apportionment of the
929 carbonaceous aerosol in Norway - quantitative estimates based on ^{14}C , thermal-optical and organic tracer
930 analysis, *Atmos Chem Phys*, 11, 9375-9394, 2011b.
- 931 Zhang, T., Engling, G., Chan, C.-Y., Zhang, Y.-N., Zhang, Z.-S., Lin, M., Sang, X.-F., Li, Y. D., and Li,
932 Y.-S.: Contribution of fungal spores to particulate matter in a tropical rainforest, *Environmental Research*
933 *Letters*, 5, No pp. given, 2010.
- 934 Zhang, Z., Engling, G., Zhang, L., Kawamura, K., Yang, Y., Tao, J., Zhang, R., Chan, C.-y., and Li, Y.:
935 Significant influence of fungi on coarse carbonaceous and potassium aerosols in a tropical rainforest,
936 *Environmental Research Letters*, 10, 1-9, 2015.
- 937 Zhu, C., Kawamura, K., and Kunwar, B.: Organic tracers of primary biological aerosol particles at
938 subtropical Okinawa Island in the western North Pacific Rim, *Journal of Geophysical Research:*
939 *Atmospheres*, 120, 5504-5523, 2015.
- 940

941 **Tables and Figures:**

942

			Mass Concentration					
			Arabitol (ng m ⁻³)		Mannitol (ng m ⁻³)		(1→3)-β-D-glucan (pg m ⁻³)	
			Rainy	Dry	Rainy	Dry	Rainy	Dry
Mass Concentration	Mannitol (ng m ⁻³)	Rainy	<u>0.839</u>					
		Dry		0.312				
	(1→3)-β-D-glucan (pg m ⁻³)	Rainy	0.000		0.003			
		Dry		0.000		0.327		
	Endotoxins (EU m ⁻³)	Rainy	0.116		0.126		0.427	
		Dry		0.012		0.113		0.103

943

944 **Table 1:** Square of correlation coefficients (R^2) comparing total mass concentration of molecular tracers945 to each other. EU: endotoxin units. Boxes colored by coefficient value (**Bold Underline** > 0.7; 0.7 > **Bold**

946 > 0.4).



		Mass Concentration								Fungal Spore Number Conc.						
		Arabitol (ng m ⁻³)		Mannitol (ng m ⁻³)		(1→3)-β-D-glucan (pg m ⁻³)		Endotoxins (EU m ⁻³)		Arabitol (spores m ⁻³)		Mannitol (spores m ⁻³)		Colony Forming Units (CFU m ⁻³)		
		Rainy	Dry	Rainy	Dry	Rainy	Dry	Rainy	Dry	Rainy	Dry	Rainy	Dry	Rainy	Dry	
UV-LIF Mass or Number Concentration	UVAPS	<u>0.732</u>	0.127	<u>0.877</u>	0.160	0.006	0.012	0.153	0.067	<u>0.483</u>	0.278	<u>0.504</u>	<u>0.571</u>	<u>0.469</u>	<u>0.491</u>	
	WIBS	FL	<u>0.554</u>	0.250	<u>0.810</u>	0.255	0.128	0.010	0.068	0.066	0.159	0.200	0.088	0.314	0.330	<u>0.737</u>
		FL1	<u>0.602</u>	<u>0.445</u>	<u>0.819</u>	<u>0.412</u>	0.042	0.001	0.090	0.012	<u>0.667</u>	0.339	<u>0.863</u>	<u>0.621</u>	<u>0.470</u>	<u>0.546</u>
		FL2	<u>0.617</u>	0.248	<u>0.843</u>	0.342	0.092	0.001	0.039	0.094	<u>0.485</u>	0.302	<u>0.442</u>	0.340	<u>0.560</u>	<u>0.543</u>
		FL3	<u>0.561</u>	0.222	<u>0.818</u>	0.251	0.124	0.008	0.071	0.065	0.178	0.181	0.104	0.306	0.367	<u>0.736</u>
		Cl1	<u>0.824</u>	<u>0.764</u>	<u>0.799</u>	0.109	0.000	0.134	0.229	0.011	<u>0.679</u>	<u>0.543</u>	<u>0.775</u>	<u>0.423</u>	0.128	<u>0.690</u>
		Cl2	0.005	0.002	0.004	0.006	0.002	0.047	0.006	0.017	0.052	0.056	0.001	0.075	0.081	<u>0.930</u>
		Cl3	0.267	0.164	0.261	0.198	0.003	0.011	0.016	0.066	0.052	0.116	0.087	<u>0.439</u>	0.262	0.383
		Cl4	0.048	0.046	0.172	0.118	0.115	0.011	0.179	0.145	0.062	0.089	0.001	0.065	0.120	0.000
	Cl _{Bact}							0.041	0.081							

947 **Table 2:** Square of correlation coefficients (R^2) comparing fluorescent particle measurements from UV-LIF instruments to measurements from
 948 molecular tracers. Columns marking tracer mass (top line) indicate correlations between time-averaged UV-LIF and tracer mass concentrations
 949 (left side), and columns marking fungal spore number indicate correlations between fungal spore number concentrations estimated from time-
 950 averaged UV-LIF and tracer or culture measurements (right side). FL1, FL2, FL3 represent individual channels from the WIBS. FL represents all
 951 particle exhibiting fluorescence in any channel. Cl1, Cl2, Cl3, Cl4 are clusters that estimate particle concentrations as a mixture of various
 952 channels (Crawford et al., 2015). Cl_{Bact} is a sum of the “bacteria” clusters Cl2-4. Boxes colored by coefficient value (**Bold Underline** > 0.7; 0.7 >
 953 **Bold** > 0.4).

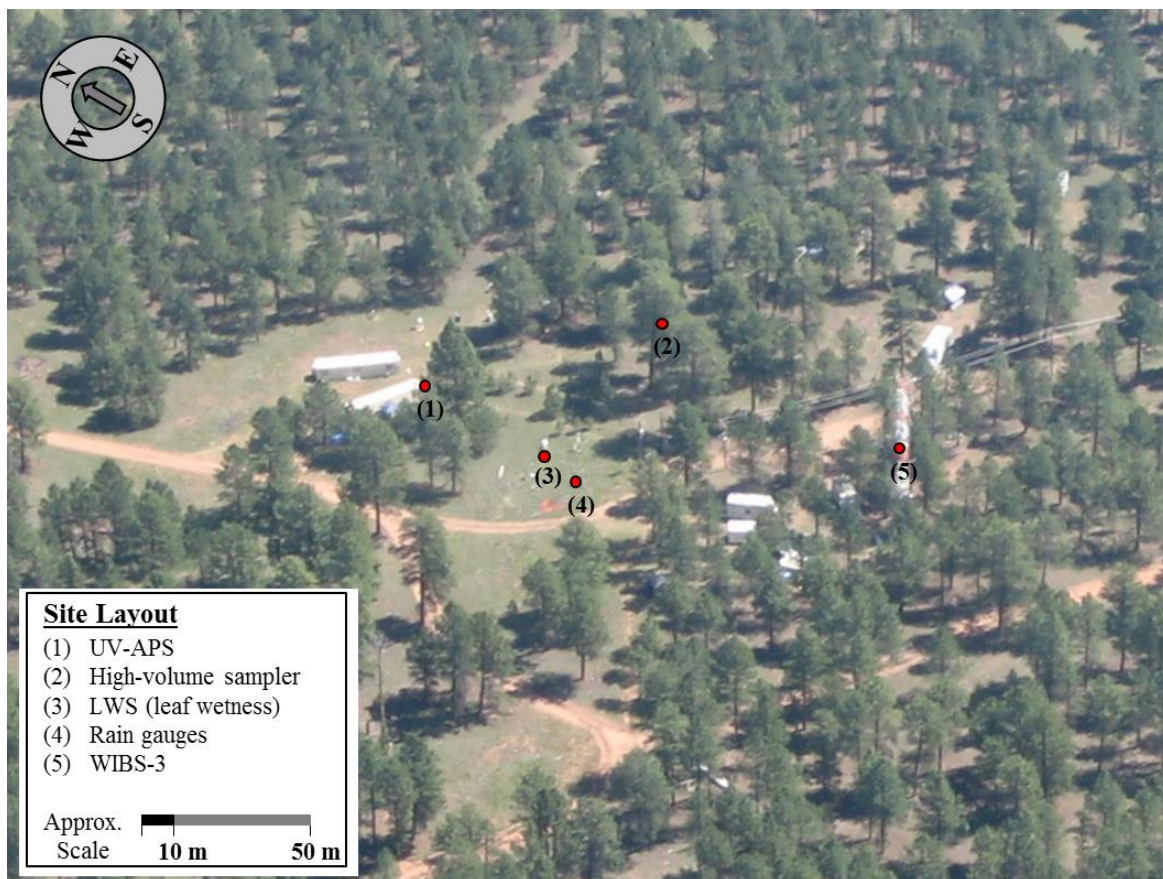


Mass Concentration							
	Arabitol (ng m ⁻³)	Mannitol (ng m ⁻³)	Erythritol (ng m ⁻³)	Levoglucosa n (ng m ⁻³)	Glucose (ng m ⁻³)	Endotoxins (EU m ⁻³)	(1→3)-β- D-glucan (pg m ⁻³)
Dry	10.6 ± 2.5 n = 18	11.9 ± 3.2 n=18	0.840 ± 0.610 n=16	14.2 ± 10.7 n=15	38.7 ± 21.3 n=18	0.192 ± 0.0970 n=18	8.8 5 ± 7.68 n=18
Rainy	35.2 ± 10.5 n=11	44.9 ± 13.8 n=11	1.12 ± 0.38 n=3	12.4 ± 19.1 n=8	73.2 ± 50.5 n=11	1.43 ± 1.22 n=10	10.6 ± 8.2 n=11
Other	20.2 ± 8.9 n=6	22.7 ± 8.3 n=6	0.664 ± 0.515 n=6	9.21 ± 1.66 n=5	56.5 ± 39.2 n=6	0.311 ± 0.159 n=6	6.08 ± 6.08 n=6
Mass Contribution (%)							
Dry	0.18 % ± 0.05 n=18	0.202 % ± 0.073 n=18	0.0.14 % ± 0.011 n=16	0.21 % ±0.17 n=15	0.67 % ±0.49 n=18		0.16 % ±0.16 n=18
Rainy	0.83 % ± 0.32 n=11	1.07 % ±0.44 n=11	0.032 % ±0.009 n=3	0.27 % ±0.41 n=8	1.60 % ±1.09 n=11		0.25 % ±0.21 n=11
Other	0.25 % ± 0.28 n=6	0.37 % ± 0.29 n=6	0.013 % ±0.015 n=6	0.15 % ±0.11 n=5	0.83 % ±0.64 n=6		0.12 % ±0.19 n=6
Fungal Spore Number Concentration (m ⁻³)							
Dry	8870 ± 2060 n=18	6890 ± 1870 n=18					
Rainy	29310 ± 8727 n=11	26430 ± 8139 n=11					
Other	16850 ± 7415 n=6	13350 ± 4863 n=6					
Fungal Spore Mass Contribution (%)							
Dry	4.81 % ± 1.36 n=18	3.72 % ± 1.12 n=18					
Rainy	22.88 % ±8.84 n=11	20.66 % ±8.49 n=11					
Other	9.80 % ± 7.67 n=6	7.31 % ± 5.60 n=6					

954 **Table 3:** Campaign-average concentrations of molecular tracers (measured) and fungal spores (number
 955 concentration estimated from arabitol and mannitol mass). Each set of data broken into wetness
 956 categories. Values are mean ± standard deviation; *n* shows the number of samples used for averaging.
 957 Fungal spore mass contribution was based on the assumption by Bauer et al. (2008b) of 33 pg spore⁻¹.
 958 Total particulate matter mass calculated from UV-APS number concentration (m⁻³) and converted to mass
 959 over aerodynamic particle diameter range 0.5 – 15 μm using density of 1.5 g cm⁻³.

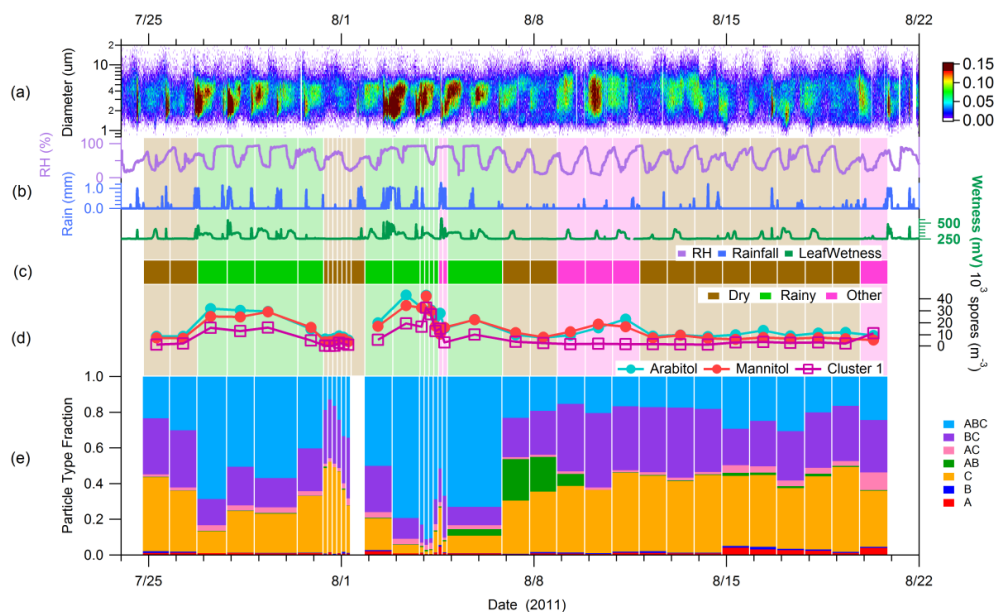


960

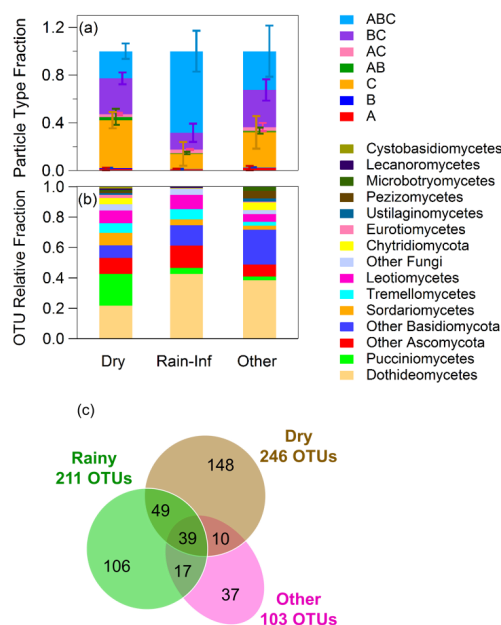


961
962
963
964
965
966

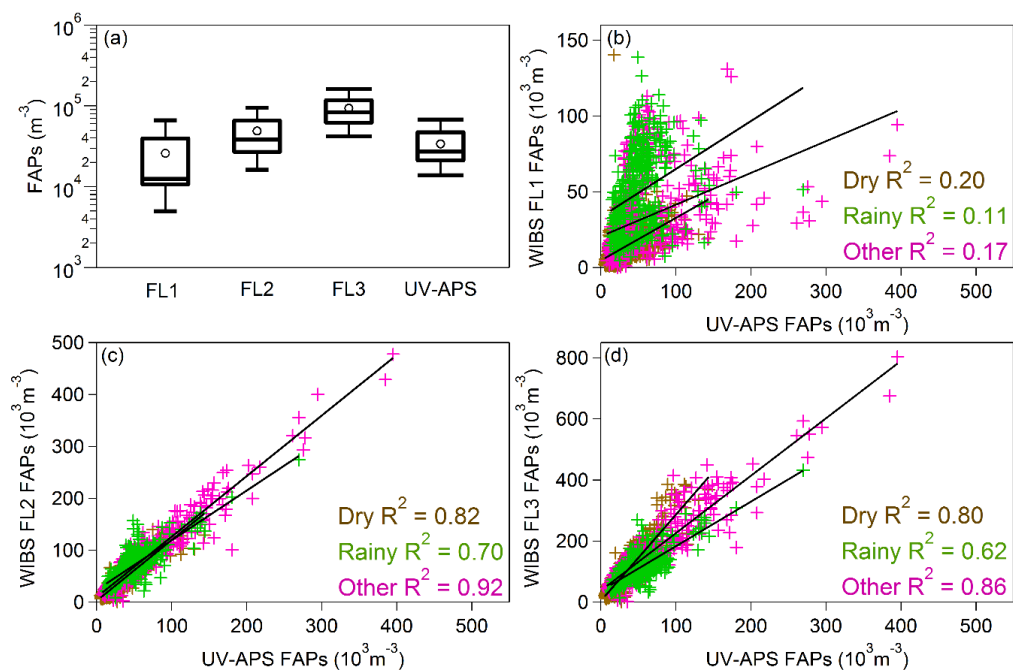
Figure 1: Aerial overview of BEACHON-RoMBAS field site at the Manitou Experimental Forest Observatory located northwest of Colorado Springs, CO. Locations of all instruments and sensors discussed here are marked and were located within a 50 m radius. Figure adapted from Figure 1a of Huffman et al. (2013)



967
968 **Figure 2:** Time series of key species concentrations and meteorological data over entire campaign. (a)
969 Fluorescent particle number size distribution measured with UV-APS instrument. Color scale indicates
970 fluorescent particle number concentration (L^{-1}). (b) Meteorological data: relative humidity (RH),
971 disdrometer rainfall (mm per 15 min), leaf wetness (mV). (c) Wetness category indicated as colored bars;
972 green, Rainy; brown, Dry; pink, Other. Bar width corresponds to filter sampling periods. Lightened
973 colored bars extend vertically to highlight categorization. (d) Colored traces show fungal spore
974 concentrations estimated from molecular tracers (circles) and WIBS C11 data (squares). (e) Stacked bars
975 show relative fraction of fluorescent particle type corresponding to each WIBS category.

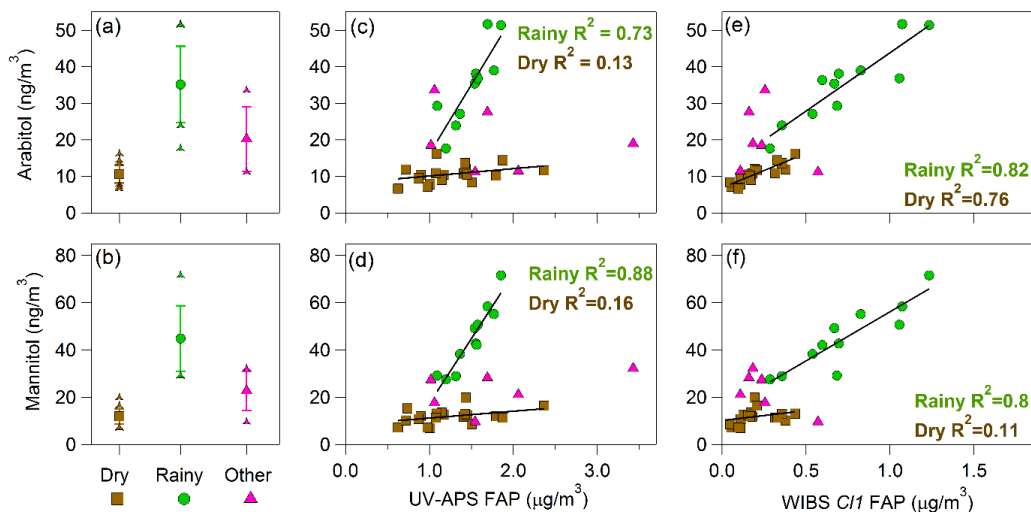


976
 977 **Figure 3:** Characteristic differences between different wetness periods (Dry, Rainy, Other). (a) Relative
 978 fraction of fluorescent particle number corresponding to each WBS category. Bars show relative standard
 979 deviation of category fraction in each wetness group (Dry, 19 samples; Rainy, 11 samples; Other, 6
 980 samples). (b, c) Distribution of fungal OTU (operational taxonomic unit) values. (b) Fungal community
 981 composition at phylum and class level with Agaricomycetes (dominant class with consistently ~60% of
 982 diversity) removed. Relative proportion of OTUs assigned to different fungal classes and phyla for each
 983 sample category shown. (c) Venn diagram showing the number of unique (wetness category specific) and
 984 shared OTUs (represented by numbers in overlapping areas) among the sample categories (Dry, 11
 985 samples; Rainy, 7 samples; Other, 3 samples). OTUs classified as cluster of sequences with $\geq 97\%$
 986 similarity. Taxonomic assignments were performed using BLAST against NCBI database. In total, 3902
 987 sequences, representing 406 fungal OTUs from 3 phyla and 12 classes were detected. Despite differences
 988 in community structure across the sample categories, phylogenetic representation appears largely similar.



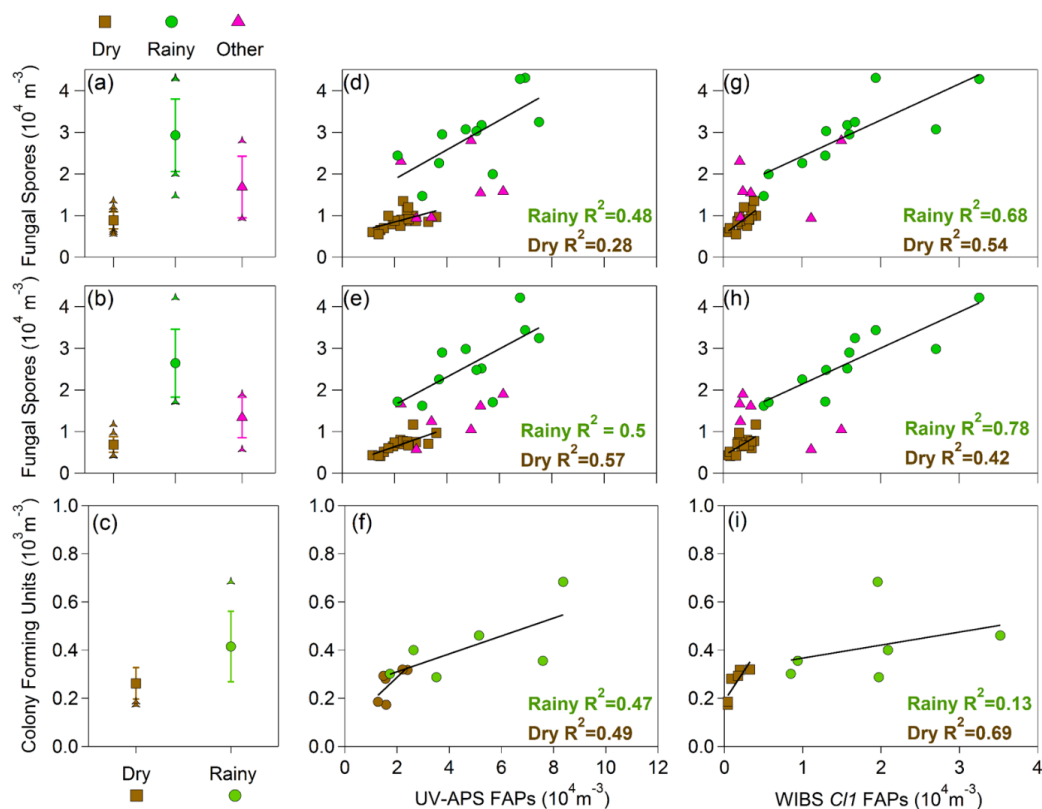
989
990
991
992
993
994
995

Figure 4: Number concentration of fluorescent particles as a function of instrument channel, averaged over entire measurement period. (a) Box-whisker plot of fluorescent particle number concentration for WIBS FL1, FL2, FL3, and UVAPS. Circle markers shows mean values, internal horizontal line shows median, top and bottom of box show inner quartile, and whiskers show 5th and 95th percentiles. (b) WIBS FL1 versus UV-APS (c) WIBS FL2 versus UV-APS (d) WIBS FL3 versus UV-APS. Crosses represent 5-minute average points. Linear fits assigned for data in each wetness category.

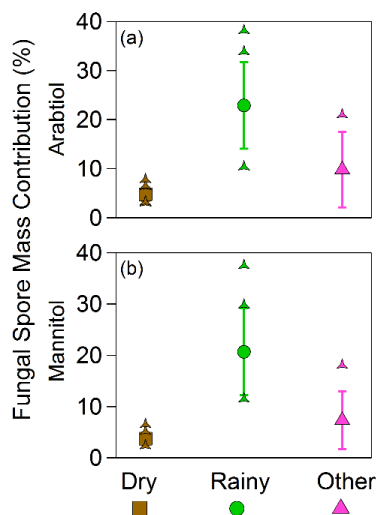


996
997

998 **Figure 5:** Mass concentrations of molecular tracers and fluorescent particles (assuming unit density
999 particle mass): arabinol – top row, and mannitol – bottom row. Average mass concentration of arabinol (a)
1000 and mannitol (b) in each wetness category. Central marker shows mean value of individual filter
1001 concentration values, bars represent standard deviation (s) range of filter values, and individual points
1002 show outliers beyond $\pm s$. Correlation of arabinol (c) and mannitol (d) with fluorescent particle mass
1003 from UV-APS. Correlation of arabinol (e) and mannitol (f) with fluorescent particle mass from WIBS
1004 Cluster 1. R^2 values shown for each fit in c, d, e, f. Linear fit parameters are shown in Table S2.



1005
 1006 **Figure 6:** Estimated fungal spore number concentration, calculated using mass of arabitol and mannitol
 1007 per spore reported by Bauer et al. (2008a). Estimates from arabitol (top row) and mannitol (middle row).
 1008 Average fungal spore concentration, calculated using arabitol mass (a), mannitol mass (b), and colony
 1009 forming units (c) in each wetness category. Central marker shows mean value of individual filter
 1010 concentration values, bars represent standard deviation (s) range of filter values, and individual points
 1011 show outliers beyond mean $\pm s$. Correlation of fungal spore number calculated from arabitol (d), mannitol
 1012 (e), and colony forming units (f) concentration with estimated fluorescent particle mass from UV-APS.
 1013 Correlation of fungal spore number calculated from arabitol (g), mannitol (h), and colony forming unit (i)
 1014 concentration with fluorescent particle concentration from WIBS Cluster 1. R^2 value shown for each fit
 1015 (right two columns). Linear fit parameters are shown in Table S3.



1016

1017

1018

1019

1020

1021

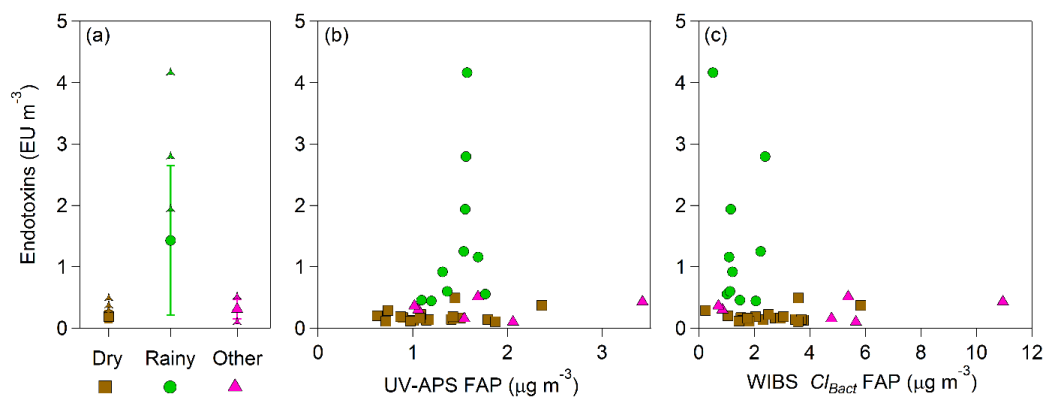
1022

1023

Figure 7: Estimated fraction of total aerosol mass contributed by fungal spores. Fungal spore mass concentration ($\mu\text{g}/\text{m}^3$) calculated separately from mannitol and arabitol concentration and using average mass per spore reported by Bauer et al. (2008b). Total particulate matter mass calculated from UV-APS number concentration (m^{-3}) and converted to mass over aerodynamic particle diameter range $0.5 - 15 \mu\text{m}$ using density of 1.5 g cm^{-3} . Central marker shows mean value of individual filter concentration values, bars represent standard deviation (s) range of filter values, and individual points show outliers beyond mean $\pm s$.



1024



1025

1026

1027

1028

1029

1030

1031

1032

Figure 8: Endotoxin mass concentration as an approximate indicator of gram-negative bacteria concentration. (a) Averaged concentration in each wetness category. Central marker shows mean value of individual filter concentration values, bars represent standard deviation (s) range of filter values, and individual points show outliers beyond mean $\pm s$. (b) Correlation of endotoxin mass concentration with estimated fluorescent particle mass from UV-APS. (c) Correlation of endotoxin mass concentration with estimated fluorescent particle mass summed from Clusters 2, 3, and 4 from Crawford et al. (2015).